

Production of highly porous Al-Ni foams by powder metallurgy using dolomite as a foaming agent.

Ana Maria Medina Ramirez

A Thesis
in
The Department
of
Mechanical and Industrial Engineering

Presented in Partial Fulfillment of the Requirements
For the Degree of Master of Applied Science (Mechanical Engineering) at
Concordia University Montreal
Montreal, Quebec, Canada

November - 2016

© Ana Maria Medina Ramirez, 2016

CONCORDIA UNIVERSITY
SCHOOL OF GRADUATE STUDIES

This is to certify that the Thesis prepared,

By: **Ana Maria Medina Ramirez**

Entitled: **“Production of highly porous Al-Ni foams by powder metallurgy using dolomite as a foaming agent”**

and submitted in partial fulfillment of the requirements for the Degree of

Master of Applied Science (Mechanical Engineering)

Complies with the regulations of this University and meets the accepted standards with respect to originality and quality.

Signed by the Final Examining Committee:

_____	Chair
Dr. I. Contreras	
_____	Examiner
Dr. M. Hojjati	
_____	Examiner (external)
Dr. M. Pekguleryuz	
_____	Supervisor
Dr. R. A.L Drew	

Approved by:

Dr. S. Narayanswamy, MASc Program Director
Department of Mechanical and Industrial Engineering

Dean A. Asif, Faculty of Engineering & Computer Science,

Date: November 28, 2016

ABSTRACT

In this study, metal foams were fabricated using Al-Ni combined with dolomite($\text{CaMg}(\text{CO}_3)_2$) as an alternative foaming agent via the powder metallurgy (PM) route. For first-time dolomite, a dual carbonate (magnesium-calcium) was found to be a highly effective foaming and an excellent stabilizing agent. It has a gradual decomposition and at different temperatures produces oxides, improving foaming conditions and expansion performance. The experimental findings showed that the addition of 7wt% of dolomite is the optimal amount for the development of well-formed pores with uniform cell distribution, spherical shape, and thick cell walls. The addition of Ni to the mixture increased the melting temperature and decreased the difference between the alloying melting point and dolomite decomposition temperature. Specific Al-Ni compositions showed appropriate viscosities for enclosing the gas as it was released. Al-10Ni and Al-15Ni were found the optimum combinations to form intermetallics which further helped stabilize the foams. Moreover, as a result of this investigation, a modification of the powder metallurgy technique was proposed, by partial-sintering the precursors before the foaming process (i.e. raising the temperature of the precursor for a period of time prior to foaming). This step allowed the formation of particle sintering, enhancing foam expansion, leading to more homogeneous porosity, cell morphology and microstructure.

The following thesis is based in one paper, which has been submitted to the journal, *Advanced Engineering Materials*.

*A mi madre, Marisol Ramírez,
por su valentía y esfuerzo, con la cual ha cambiado nuestra
historia*

*y a mi hermana, Ivonne Medina,
por su ejemplo, he forjado mi camino.*

Ustedes son la luz de mi vida.

Acknowledgements

I gratefully acknowledge my supervisor, Professor Robin Drew for his support, encouragement, and leadership during the entire master program. I have been fortunate to work with a supervisor who is both knowledgeable and approachable and has made a strong team between all his students, making it a pleasant work environment.

I am deeply grateful to Ramona Vintila, and Dr. Ehsan Rezabeigi for their collaboration, support, modesty, and the generous way they share their wide knowledge with me, influencing both my skills and my taste for research. Thank you, Ramona Vintila for your guidance when I felt lost and the confidence placed in me. Thank you Dr. Ehsan Rezabeigi for your contribution of valuable directions and suggestions throughout the entire process, I have learned from you, patience, commitment, and dedication for what we do.

I would like to thank Ryan Cunningham for helping me to find my path, for encouraging me to study in the materials field and for always seeing the best in me as an engineer. Special thanks to my friends Hamid Hamidi and Mohammad Mahdipoor for enriching my student experience at Concordia. Thank you to Ali Louati for his constant motivation, for helping me to fix the equipment, and for never letting me down.

Last, but by no means least, my deepest gratitude to my family for all their support, patience, love and encouragement over the last two years.

TABLE OF CONTENT

1. INTRODUCTION.....	1
2. LITERATURE REVIEW.....	4
2.1 METAL FOAMS – CELLULAR MATERIALS.....	4
2.2 PRODUCTION METHODS OF CELLULAR METALS	5
2.2.1 Metal Vapour Foaming.....	5
2.2.2 Powdered Metal Foaming.....	6
2.2.3 Liquid Metal Foaming.....	7
2.2.4 Metal Ionic State Foaming	9
2.3 POWDER METALLURGY (PM)	10
2.3.1 Influence of Powder Compaction.....	11
2.3.2 Heat Treatment	12
2.3.3 Sintering.....	13
2.4 FOAM STABILITY	14
2.4.1 Aqueous Foams and Surfactants.....	15
2.4.2 Particle Stabilized Foams	16
2.4.3 Role of Blowing Gas or Foaming Agent on Foam Stability	16
2.5 BLOWING AGENTS.....	17
2.5.1 Hydrides as Blowing Agents	18
2.5.2 Carbonates as a Blowing Agents	18
2.5.3 Dolomite as a Foaming Agent.....	19
2.6 EFFECT OF ALLOYING ELEMENTS IN ALUMINUM	21
2.6.1 Al-Ni Intermetallics.....	22
2.7 PROPERTIES OF ALUMINUM FOAMS	23
2.7.1 Mechanical Properties	23
2.7.1.1 Compression Behavior	24
2.7.1.2 Energy Absorption	25
2.7.1.3 Three-point bending test.....	25
2.8 APPLICATIONS.....	26
3. OBJECTIVES	28
4. EXPERIMENTAL PROCEDURE	29

4.1	MATERIAL SELECTION AND PREPARATION.....	29
4.2	POWDER MIXING	30
4.3	COMPACTION (Preparation of precursors).....	31
4.4	PRECURSORS PARTIAL-SINTERING	32
4.5	FOAMING PROCESS	32
4.6	CHARACTERIZATION OF THE FOAMS	33
4.6.1	Scanning Electron Microscopy (SEM).....	33
4.6.2	X-Ray Diffraction (XRD).....	34
4.6.3	Differential Scanning Calorimetry (DSC) and Thermogravimetric Analysis (TGA)	34
4.6.4	3D-Optical Microscopy	35
4.7	MECHANICAL TESTING.....	35
4.7.1	Compression Testing.....	35
4.7.2	Three-point bending flexural test	36
5.	PRODUCTION OF HIGHLY POROUS AL-NI FOAMS WITH DOLOMITE AS FOAMING AGENT VIA THE POWDER METALLURGY TECHNIQUE	39
5.1	ABSTRACT.....	39
5.2	INTRODUCTION.....	39
5.3	EXPERIMENTAL	42
5.3.1	Precursors fabrication	42
5.3.2	Foaming procedure	44
5.3.3	Characterisation techniques	44
5.4	RESULTS.....	45
5.4.1	Optimum concentration of additives.....	45
5.4.2	Foaming behavior of the partially-sintered precursors	47
5.5	DISCUSSION	49
5.5.1	Foaming mechanism	49
5.5.2	Influence of the Partial-Sintering step on foam evolution.....	51
5.5.3	Influence of Nickel and Dolomite additions on the foaming process.....	55
5.5.3.1	Influence of Nickel additions	55
5.5.3.2	Influence of Dolomite Content.....	56
5.5.3.3	Pore Morphology, Microstructure and Phase analysis.....	57
5.6	CONCLUSIONS.....	61
6.	MECHANICAL CHARACTERIZATION OF AL-NI FOAMS.....	63

6.1	Compression Test.....	63
7.	CONCLUSIONS.....	68
8.	FUTURE WORK.....	72
9.	REFERENCES.....	73

List of Figures

Fig. 2.1: Nickel reticulated-polyurethane-foam	6
Fig. 2.2: Magnified view of metal foam surface produced by powdered metal foaming	7
Fig. 2.3: Foaming of Aluminum by the melt gas injection method	8
Fig. 2.4: Metal ionic state foaming process.....	9
Fig. 2.5: Powder metallurgical process chain.....	10
Fig. 2.6: Powder metallurgy foaming process.....	11
Fig. 2.7: Sintering Stages.....	13
Fig. 2.8: Scheme of an aqueous surfactant at the interface between two cells.....	15
Fig. 2.9: Binary Ni–Al equilibrium phase diagram.....	22
Fig. 2.10: Stress-Strain curve obtained from a uniaxial compressive load.	24
Fig. 2.11: DUACEL aluminum foam used for energy absorbers and thermal energy absorbers for medical laser applications	27
Fig. 4.1: Graphic description of the Laser Expandometer.....	32
Fig. 4.2: Schematic of MTS compression machine.....	36
Fig. 5.1: Scanning electron microscopy (SEM) images of the starting materials: a) Aluminum, b) Nickel and c) Dolomite.....	43
Fig. 5.2: Porosity levels (a) and volume expansion (b) of cellular specimens produced from precursors containing 0wt% Ni (pure Al), 5wt% Ni (Al-5Ni), 10wt% Ni (Al-10Ni) and 15wt% Ni (Al-15Ni) with increasing dolomite content of 3, 5, 7 and 10wt%.....	46
Fig. 5.3: Macrostructure of the resulting foams obtained from partially-sintered precursors of various dolomite and nickel contents.....	47
Fig. 5.4: Comparison of foaming evolution of Al-15Ni with 7wt% dolomite precursor in the “as-compacted” vs partially-sintered state	48
Fig. 5.5: Schematic representation of the foaming process and evolution of Al-10Ni foam.	50
Fig. 5.6: Fracture Surfaces of Al10Ni with 7wt% compacts with 98% of the theoretical density: “as-compacted” (a; b-higher magnification); Partially-sintered I at 450°C, 15 min (c; d – higher magnification) Partially-sintered II at 450°C, 20 min (e; f – higher magnification)	53
Fig. 5.7: Pore morphology for foams obtained from precursors containing 5wt%Ni (Al-5Ni); 10wt%Ni (Al-10Ni) and 15wt% Ni (Al-15Ni) with 7wt% dolomite	59
Fig. 5.8: Microstructure of Al-10Ni Foam with 7wt% (a) Pore morphology, (b) Plateau Border zones and (c) Internal cell surface	60
Fig. 6.1: Machined specimens at the maximum level of expansion of Al-10Ni 7 wt.% Dolomite	64
Fig. 6.2: Stress-Strain Curves of Al10Ni and Al15Ni with dolomite (7 and 10wt%).....	65

List of Tables

Table 2.1: Summary of the several manufacturing processes for cellular metallic structures.....	5
Table 2.2: Summary of the results of studies of aluminum foams using dolomite as a foaming agent.....	20
Table 4.1: Summary of the powders used according to supplier, mesh size, level of purity and oxygen content.....	29
Table 4.2: Powders size analysis.....	30
Table 4.3: Mixture composition and concentration matrix.....	30
Table 4.4: Powder Pressing Parameters.....	31
Table 5.1: TRS data of Al-10Ni with 7wt% dolomite precursor in the “as-compacted” and partially-sintered state.....	52
Table 6.1: Density, relative density and compressive properties of the tested samples.....	66

1. INTRODUCTION

High-quality, low-density materials are becoming formidable players in multiple industrial applications. Due to their unique properties, metal foams are attractive materials for structural engineering and design applications. Overtime, several manufacturing processes have been developed and classified [1, 2]. However, the main limitations with metal foams remain the same for all materials selection criteria: the overall cost, the stability, and the process control. Certainly, these limitations are found in each manufacturing process described.

Powder Metallurgy (PM) for instance, is an indirect technique, consisting of a mixture of metal powders with a suitable foaming agent which is a challenging process to control and can be costly. The systematic procedure for creating a metal foam by PM is mainly the mixing of different metals powder with an agent capable of releasing gas (usually through decomposition). The combination of diverse metals brings the ability to tailor and obtain valuable foam properties [3]. After a well-distributed powder blend has been achieved, it is necessary to compress the blend until a dense precursor is obtained. This foamable precursor goes through a heat treatment until the metal becomes a viscous semi-liquid mass and the foaming agent undergoes decomposition, at this point, a foam will have been formed [4].

Suitable closed cell foams have been produced by the PM route implementing TiH_2 and other hydrides as foaming agents. The latter is expensive and dangerous to handle. Recent studies have focused on the replacement of hydrides with new inexpensive agents such as carbonates. Carbonates are naturally occurring minerals. Due to their composition, they are capable of decomposing at high temperatures to form oxides. They are expected to be effective foaming compounds with the ability of achieving similar product properties to hydrides and hence satisfactory results. Dolomite ($\text{CaMg}(\text{CO}_3)_2$), for instance, is a carbonate that has been attempted previously as a foaming agent but with limited success. Upon decomposition, it releases carbon dioxide gas (CO_2). It offers significantly lower cost, a more precise stabilization temperature [5], produces a finer cell structure and has several other advantages. The chemical composition of dolomite, also produces oxides such CaO and MgO , which provide stability in the final stages of foaming, avoiding the need for the addition of ceramic particles. However, in the literature, there are just a few studies about dolomite used as a foaming agent, and despite its multiple advantages, those studies have reported a low range of porosities and small pore size. As it currently stands, dolomite has not shown itself to be a suitable replacement for titanium hydride (TiH_2) as a foaming agent.

Generally, the production of aluminum foams by the PM has proven challenging due to the discrepancy of temperatures between the aluminum melting point and the decomposition of the foaming agent. This discrepancy is considered a major factor for reduced foam expansion and absence of pore structure uniformity [6]. In the present study, Ni was added to the Al matrix with dolomite. Having an Al-Ni matrix reduces the mismatch of temperatures and produces a complete system for the production of highly porous foams. The melting point of the metallic matrix is

increased to above 700°C and allows the formation of Al-Ni intermetallics. Additionally, a partial-sintering step is suggested in order to reduce minimum values of residual porosity and to accelerate the driving forces in the foaming stage. This final system Al-Ni + dolomite presents favorable thermodynamic behavior to enhance foaming conditions and final microstructure. It can modify the foam behavior by (1) improving foam expansion, (2) increasing pore connectivity and (3) stabilizing the foam in terms of homogenizing pore size and pore distribution.

2. LITERATURE REVIEW

2.1 METAL FOAMS – CELLULAR MATERIALS

In the field of materials sciences and engineering, the meaning of the term FOAM is defined as a material consisting of a well dispersed concentrated gas phase in a solid phase, even though the primary concept describes a gaseous phase immersed in a liquid phase. Thus, words resembling ‘solid foams’ or ‘cellular materials’ would be more appropriate to describe the sequence of cells arranged in an interconnected porous structure.

Nowadays excellent advanced materials with that porous structure are well-known to exhibit important physical and mechanical properties, for instance, compressive strengths combine with good energy absorption along with high thermal conductivity. These porous low-density cellular materials are found both naturally and manufactured. In nature, foams are anisotropic cells like bones, sponge, wood, corals and bee honeycombs [7,8]. Industrialized foams are extensively used at the moment in the form of shaving cream, soaps, cleaning agents, ice cream, packaging, thermal insulation and in many commercial mineral manufactured products.

To clarify the meaning of foam, it is principally any material with the ability to trap gas bubbles from its liquid state. Solid metal foams are materials that can be composed of 40% to 90% volume of gas. They are being developed and classified not only according to their processing techniques but also according to their applications [7].

2.2 PRODUCTION METHODS OF CELLULAR METALS

There are different routes for manufacturing metal foams, principally, depending on the state in which the metal is found to be treated. In general, the main groups of production processes can be classified as vapor deposition processes, melt processes, powdered metal processes, and metal ion deposition processes. Banhart has presented an entire study of several techniques [1], which are summarized in Table 2.1.

Table 2.1: Summary of the several manufacturing processes for cellular metallic structures [1]

CELLULAR METALS			
Metal Vapour	Powdered Metal	Liquid Metal	Metal Iones
* Vapour deposition	<ul style="list-style-type: none"> * Direct foaming with gas * Direct foaming with blowing agents * Gasars * Powder Metallurgy * Casting * Spray forming 	<ul style="list-style-type: none"> * Sintering of hollow spheres * Gas entrapment * Slurry foaming * Pressing around fillers * Sintering of powders or fibres * Extrusion of polymer/metal 	* Electrochemical deposition

2.2.1 Metal Vapour Foaming

Metal foams manufactured from gaseous metallic materials are open cell structures. For its production, a cellular precursor in solid form is required to define the shape of the cellular material

to be formed, for example, a reticulated polymeric foams. In this approach, a metal vapor coats the surface of the precursor up to a certain thickness, creating a negative copy of its structure. The actual precursor is removed by thermal or chemical treatments [7]. Nickel foams are produced by chemical vapour deposition using a reticulated polyurethane precursor as illustrated in the figure below:

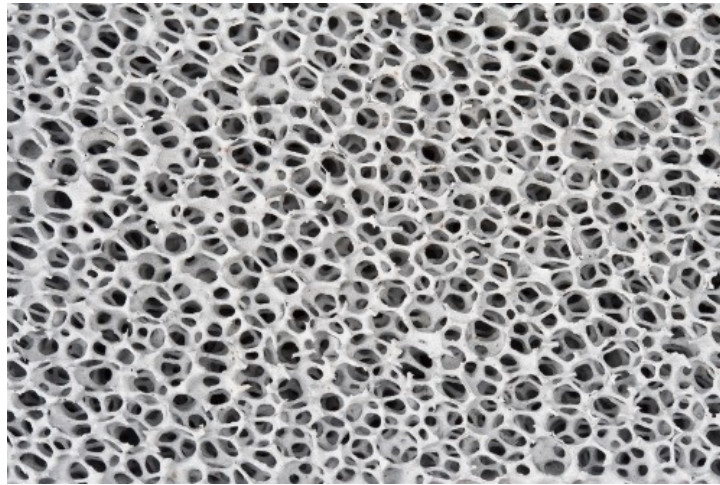


Fig. 2.1: Nickel reticulated-polyurethane-foam [9]

2.2.2 Powdered Metal Foaming

Cellular structures can be produced from metals using powder precursors. Throughout the manufacturing process, the powder remains in the solid state and only undergoes sintering. Powdered metal foams have generally close pores morphology. The formation of quasi-spherical pores is a notable characteristic of this foaming method. Principally, the approach is based on two steps: compaction or moulding and sintering; however, it has been proven that slip reaction foam sintering can be employed to produce metal foams at room temperature [10]. Furthermore, an

alternative manufacturing process involves capturing the gas in a powder compact utilizing space-holding fillers or hollow spheres [8].

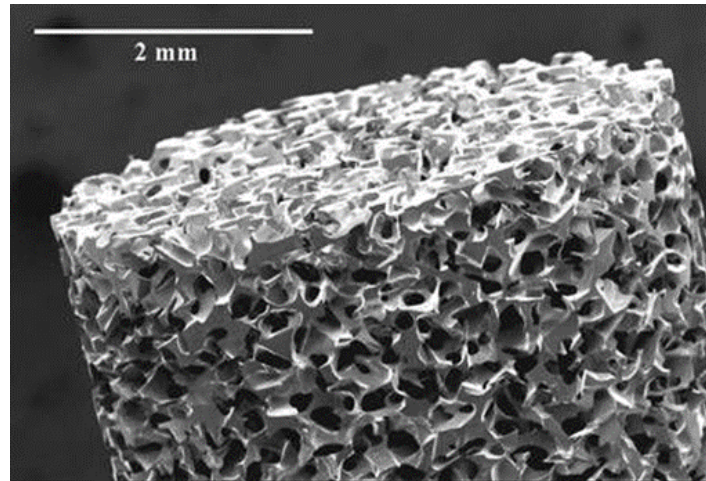


Fig. 2.2: Magnified view of metal foam surface produced by powdered metal foaming [11]

2.2.3 Liquid Metal Foaming

Liquid metal foaming for producing cellular structures is an important approach that involves melting the metal or alloy and injecting bubbles. This technique is often used on large scales in industry due to its economical production. It is one of the most cost-effective and viable processes, allowing the production of large amounts of high-quality metal foams. The manufacturing procedure depends on the incorporation method of the blowing agent or gas. It can be done by injecting a gas directly into the liquid metal, by creating a saturation of gas in the liquid by adding blowing agents to the molten metal, or by precipitating the gas which is already dissolved in the liquid [8].

Aluminium liquid metal foaming has three stages for the production of the foam, in the first stage, the aluminum melt receives additions of ceramic particles such as silicon carbide to stabilize the reaction and to enhance the viscosity of the melt (usually 5-15 vol.% is added) [12]. In the second stage, the liquid metal foams by injecting the gas into the melt, typically argon, nitrogen, or air. As it shows in Fig. 2.3:

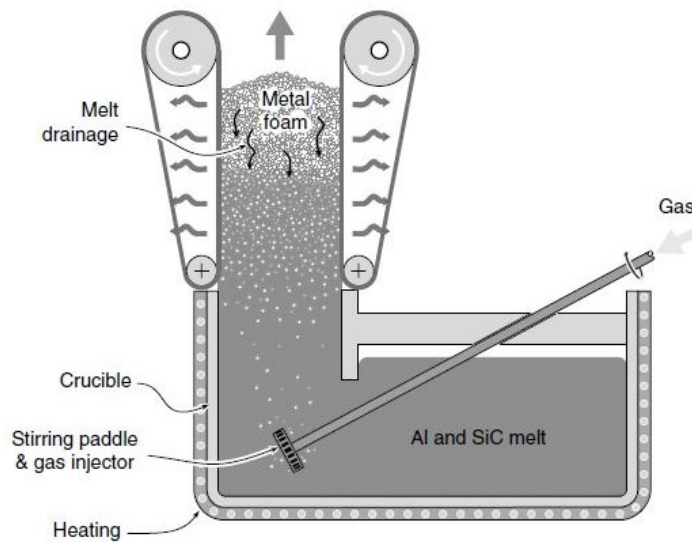


Fig. 2.3: Foaming of Aluminum by the melt gas injection method [13]

This gas is incorporated through rotating impellers generating fine bubbles and distributing them constantly. In the third stage, the gas bubbles float out of the melt and the remaining liquid films between the bubbles drain out. On one of the side of the melt, a carrying medium is located to pull out the dry foam permitting it to cool down and solidify.

As an alternative to injection, a blowing agent can be added to the melt. High temperature causes the blowing agent to decompose and then release the gas. Nevertheless, difficulties with uniform

distribution of the blowing agents as well as ceramic particles in the melt create challenges in the production of foam by this process [7].

2.2.4 Metal Ionic State Foaming

The metal ionic technique for production of metal foams is based on electrochemical deposition which is comparable to the vapor deposition technique. This method creates foams with open porosity. An electrically conductive polymer precursor is placed inside an ionized electrolyte which has been charged with negative bias. The metal ions are deposited on the surface of the precursor until a desirable thickness has been achieved. The chemically conductive polymer is removed afterwards by a thermal treatment [7].

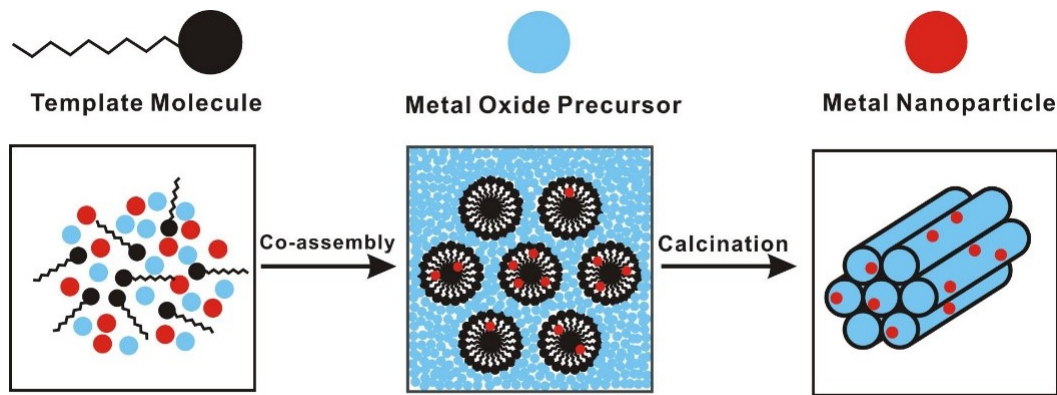


Fig. 1.4: Metal ionic state foaming process [14]

2.3 POWDER METALLURGY (PM)

Powder metallurgy is an indirect technique, consisting of a mixture of metal in powder form with a suitable blowing agent. It was first developed at the Fraunhofer Institute in Bremen and Bratislava University in partnership with the Karmann Society.

This technique is generally known for the production of aluminum foams, however, recent studies have intensified in producing titanium-nickel and steel foams [13,15]. The powder metallurgy technique is represented schematically in Fig. 2.5.

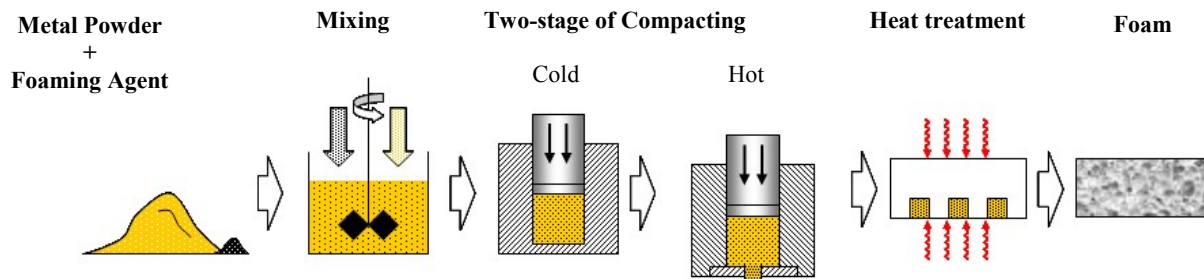


Fig. 2.5: Powder metallurgical process chain [16]

The process begins with a metal powder mixture with a blowing agent (alloys powders bring different properties to the mixture). The presence of the blowing agent embedded in the blend is a crucial step in the foaming process. The well-distributed powder-blend is compressed until a green compact is obtained. To ensure minimum voids or porosity levels inside the compact, the compaction has to reach values close to the theoretical density [17] (the most common compacting technique is cold pressing). The compression is followed by a heat-treatment at temperatures below the melting point of the matrix leading to the metal powder sintering. At this point, the foaming process begins. Finally, a continuous increase of the precursor temperature is necessary

for the metal to become a viscous semi-liquid mass and the foaming agent to undergo decomposition [1]. The gas generated from the decomposition becomes trapped and expands, producing pores and creating the foam.

Powder metallurgy has an incredible advantage over the other techniques; it allows foaming inside of a mould of different shapes. Having the possibility of creating a net-shaped product in mould of desirable geometries reduces the requirement of extra procedures such as machining.

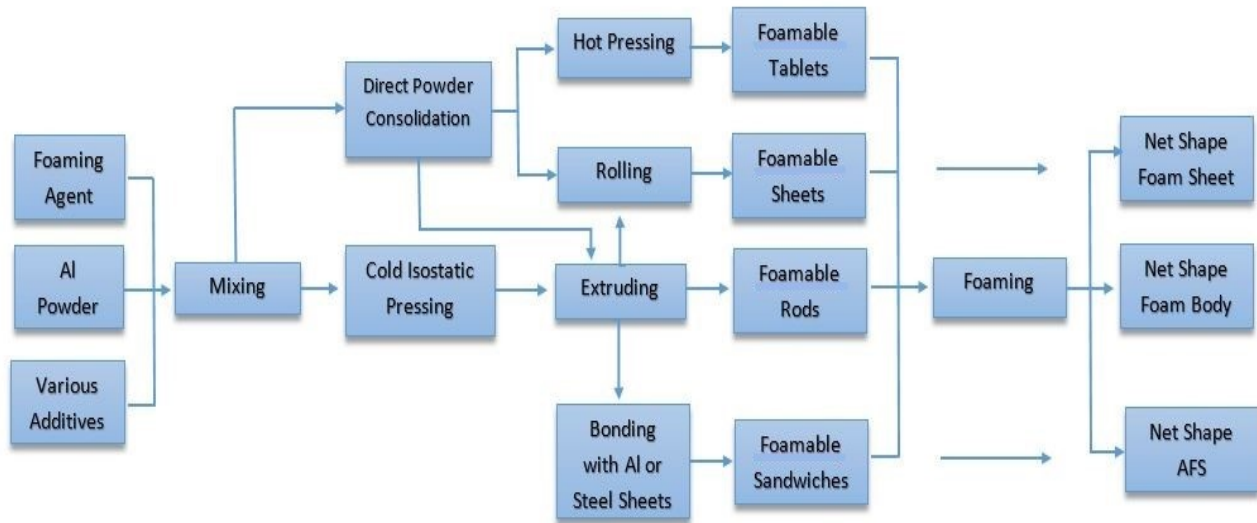


Fig. 2.6: Powder metallurgy foaming process [18]

2.3.1 Influence of Powder Compaction

Cold pressing, hot pressing, powder rolling or extrusion are methods for achieving good compact density with the powder metallurgy technique. Precise pressures for compaction are directly

related to the quality of the final product. This step has to ensure the minimum level of residual porosity present inside the compact. For this reason, some metals or alloys require additional hot pressing. This can be also employed as an initiation of the sintering stage prior to foaming [1, 18] ensuring good powder-particle bonding.

The desirable result from compaction achieves close to theoretical density. As reported by Kennedy [19] and Asavavisithchai [20] favorable compaction levels of at least 94% of the theoretical density are necessary for obtaining good foams. This eliminates internal porosity, avoids premature gas escape through the pores of the compact. Moreover, satisfactory compaction prevents frequent defects such as crack formation along powder boundaries.

2.3.2 Heat Treatment

Heat treatment is the last stage of producing metal foams by powder metallurgy route. This process takes place at a temperature close to the melting point of the alloy. The exposure to temperature decomposes the blowing agent which is embedded in the molten or semi-molten metal matrix. The gas generated from that decomposition forces the compact precursor to expand, therefore multiple pore structures nucleate and emerge creating the foam [1]. The main objective is to achieve sufficient liquid from partial melting of the matrix, while the gas evolves gradually; causing a progressive expansion by the formation of pores [21]. During expansion, rupture of cell walls of the foam occurs at the moment when the thicknesses of the walls in the metallic matrix are below a critical thickness [22]. The level of expansion has three variables that influence directly the result of the foam; temperature, size of the precursor and holding time (varies from some seconds to

more than a few minutes) [1]. In terms of the maximum expansion that a foam can achieve depends on the amount of blowing agent added in the precursor, the temperature, and, heating rate.[23]

2.3.3 Sintering

One of the most effective methods of producing porous metallic foams is the sintering of powdered metals. Sintering is a subsequent heat treatment of compacted powdered metals and is done at a temperature below the melting point to fuse the particle. Sintering usually takes 1 to 2 hours and is often done in an inert atmosphere or in a vacuum to eliminate the possibility of surface oxidation. The production of good foam is associated with the density of the sintered metal. Experiments have shown that theoretical density at least of 94% is desirable for low residual porosity and encapsulation of more blowing gas [20][19].

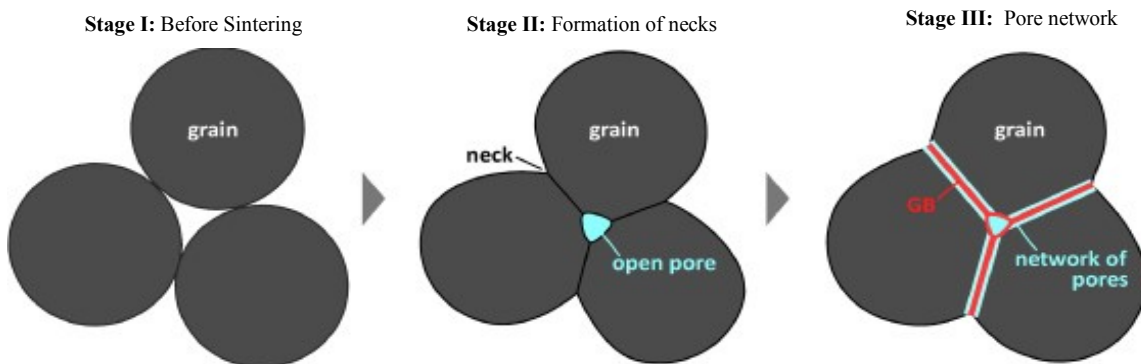


Fig. 2.7: Sintering Stages [25]

Making metal foams from aluminum alloy powders can be a big challenge due to the formation of surface oxide impeding the process of sintering between particles. But this obstacle can be solved

by deforming the particles by a continuous compression until the oxide films are ruptured and metallic bonding occurs.

2.4 FOAM STABILITY

To analyze the stability of a foam, it is essential to recognize that foams by nature are thermodynamically unstable structures due to their high surface free energy [6]. Therefore, the concept of foam stability only indicates to kinetic stabilization resulting from retarded foam collapse. Mechanisms that come into play during this degradation process are as follow: a) drainage which is caused by gravity and pressure differences, which forces the metal to collect as a pore-free liquid at the bottom of the mold; b) coalescence occurs when a cell wall disappears due to instability; and c) subsequent coarsening which forces the diffusion of gases to increase the size of cells [24]. Many forces have been found to be the culprits causing foam instability such as gas pressure, gravity, surface tension, and viscosity. Gravity causes the drainage phenomenon while surface tension and the capillary force causes thinning of the cell walls. Interaction of all these forces creates bubble instability, consequently an equilibrium of these interacting forces is important for foam stability [2].

In addition, it is impossible to foam pure aluminum because it has an insufficient bubble stability and they rupture instantaneously upon arrival at the surface [8, 26]. Several solutions have been proposed to inhibit the above phenomenon like enhancing the viscosity of the melt and addition of particles that act as the stabilizers for stable foam generation [27].

2.4.1 Aqueous Foams and Surfactants

Liquid or aqueous foam is a two-phase system in which gas bubbles are enclosed in liquid and able to maintain both of these phases into one integral system, to this end some chemical agents are required. These are organic molecules and are called surfactants because of their concentration and activeness on surfaces and liquid films. Due to their amphiphilic nature, they lower the surface tension or increase the viscosity at the liquid-gas interface by arranging themselves in a monomolecular arrangement. This arrangement serves several purposes; it not only increases the elasticity of the films thus retarding the rupturing effect but also causes the interfaces to repel each other thereby thickening the cell walls and decreasing the chances of liquid drainage [28].

Increased concentration of surfactants has been found to increase the stability of foams up to a certain limit. As long as there is room for surfactants to create monolayers on the liquid-gas interface, stability of foam is increased by increasing their concentration.

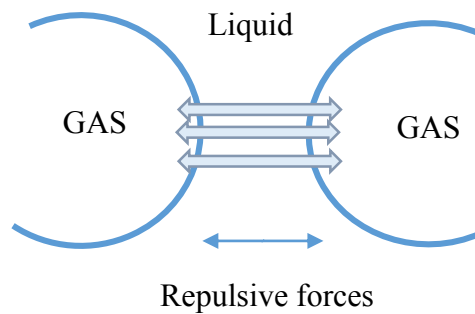


Fig. 2.8: Scheme of an aqueous surfactant at the interface between two cells [28]

2.4.2 Particle Stabilized Foams

There is an alternative approach to inhibit some of the major phenomena causing foam instability other than the use of surfactants for use at high temperatures in metals and alloys. Researchers have found that the addition of particles like SiC, Al₂O₃ or TiB₂ can stop the drainage process of liquid metal by their accumulation at the gas/liquid interface, increasing viscosity and by creating a disjoining pressure similar to surfactants [29]. It has been found that the addition of these particles can stabilize the metal foams only if the following parameters are controlled: concentration (3 vol % to 10 vol %), proper wetting, contact angle (20° to 90°) and particle size (up to 3μm) [30].

2.4.3 Role of Blowing Gas or Foaming Agent on Foam Stability

In addition to the inclusion of surfactants and ceramic particles, blowing an oxidizing gas can also enhance foam stability. Some combination of gases, such as air and other gas mixtures can increase the elasticity of the films. Their monomolecular arrangement at the liquid-gas interface decreases the surface energy of the film and delays film rupture. Some gases are found to be undesirable for this purpose for example nitrogen, hydrogen, and argon because they contain very low levels of oxygen and form only a very thin oxide film leading to film rupture and, as a consequence, more drainage. Oxygen has proved itself to be a strong candidate for this purpose because it forms thick oxide layers of up to 30nm which in turn also increases the bubble stability as well as the cell wall stability [31].

Different cell structures are obtained by using diverse foaming agents such as hydrides and carbonates. These structures are determined by two factors: decomposition temperature and type of gas released. Because of having higher decomposition temperatures than hydrides and due to the slow release of CO₂ gas upon decomposition, carbonates and, especially dolomite among carbonates, stabilizes, forms oxides in the cell walls and is more effective than hydrides. The presence of and homogeneous dispersion of solid particles in Al precursor also add to the advantage of carbonates being better foaming agents causing increased overall stability of metallic foams.

For instance, dolomite compared with hydrides forms smaller cell sizes which lead to a nearly insignificant melt drainage. The absence of a melt flow and high surface viscosity cause the cell faces to remain narrow, hence stabilizing them. Dolomite particles are wettable in aluminum due to the presence of interfacial compatibility with the Al matrix [32]. All these factors lead to more stable cell walls in the foam structure.

2.5 BLOWING AGENTS

For successful metal foaming, a crucial step is to introduce and embed a blowing agent into the cross section of compacted metal precursor because this is the material that is responsible for the creation of the foam structure by decomposing and releasing gas upon the application of heat. Concerning the achievement of a good quality of metal foams, it is very important to find the right match of temperatures between the melting point of the metal and decomposition of foaming agent otherwise, it might be detrimental to the foam metallic matrix which is undesirable [33, 34].

So far, chemicals such as metal hydrides, carbonates, organic polymers and other effervescence compounds are commonly used blowing agents but some of them are difficult to handle and expensive. Some researchers have been able to find promising materials such as dolomite $\text{CaMg}(\text{CO}_3)_2$ that releases CO_2 , producing less expensive foams than hydrides [35, 4].

2.5.1 Hydrides as Blowing Agents

Hydrides such as TiH_2 , ZrH_2 and MgH_2 are commonly used blowing agents for the production of suitable closed cell foams. Upon decomposition, they produce an excess amount of hydrogen at low temperatures which react with the precursor metal [37]. Although H_2 based foaming agents impart better mechanical properties due to the spherical shape of pores, but there are also a few problems posed by the hydrides during the foaming process: they are expensive, and their decomposition temperature is not well-defined which depends upon several factors like the size of hydride particles, heating rate and amount of surface oxidation [38]. In addition, hydrogen gas is not favoured because it causes frequent cell wall ruptures resulting in draining of the liquid metal.

2.5.2 Carbonates as a Blowing Agents

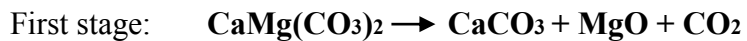
Carbonates are minerals that contain polyatomic ions (CO_3^{2-}). When carbonates combine with metals, they form insoluble compounds and upon decomposition, give off CO_2 which acts as a blowing gas during the metal foaming process. Among many carbonates, MgCO_3 , CaCO_3 , and dolomites $\text{CaMg}(\text{CO}_3)_2$ are considered to be the most suitable foaming agents for aluminum alloy

precursors because of the large generation of CO₂ accompanied by residual solid particles (such as CaO, and/or MgO), which not only help the stabilization of the foam suspension, but also enhance the melt viscosity [5].

Carbonates act as better foaming agents for several reasons. They have a higher decomposition temperature than hydrides, eliminating pre-processing or pre-treating in order to encapsulate the gas from the decomposition and to avoid its premature escape. The temperature of decomposition of some carbonates is closer to the melting temperature of pure aluminum which is also desirable. Upon reacting with Al, carbonates tend to form a small solid reaction layer during the first stages of the foaming process, [40] which is also responsible for cell stabilization. In addition, the natural oxidation process inside the material and of external surfaces also helps to stabilize the cell walls inside foams so that they do not tend to collapse immediately after the completion of the foaming process [41].

2.5.3 Dolomite as a Foaming Agent

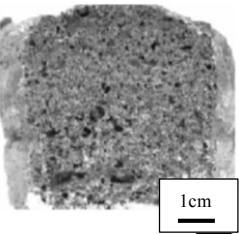
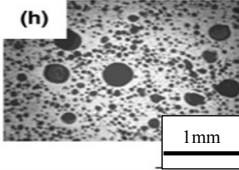
Dolomite (CaMg(CO₃)₂) as a natural mineral is a dual carbonate between calcium and magnesium. Its chemical decomposition is more gradual than hydrides and more suitable for metals with higher melting temperatures. The thermal decomposition of dolomite is a 2-stage process that follows this behavior:

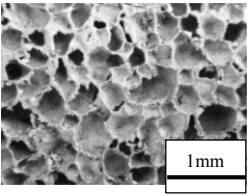


In the first stage, dolomite decomposes into calcium carbonate, magnesium oxide, and carbon dioxide. In the second stage, there is a further decomposition, and the calcium carbonate decomposes into calcium oxide and carbon dioxide. The decomposition behavior of dolomite is also different from other carbonates, it leads to the formation of thin oxide films due to the reaction of CO₂ with aluminum melt which not only increases the mechanical stability of the cell but also the overall expansion of the foam [32]. Some other notable advantages of using dolomites are: low cost, precise stabilization temperature, and its effectiveness [42].

Some studies have reported the use of dolomite as a foaming agent for the production of aluminum foam, employing powder metallurgy and melt processing. However, the foams obtained from these studies have shown common characteristics: small pore size, heterogeneous cell structure, and medium porosity levels. Such results have not yet made them competitive with foams produced with TiH₂.

Table 2.2: Summary of the results of studies of aluminum foams using dolomite as a foaming agent

Process	Metals used	Dolomite content (wt%)	Average Porosity (%)	Average Pore Size (mm)	Reference	Image
Melting	Al	0.15-3	71.4	1.3	Ref [43] Ref [35]	
PM and melting	AlSiCu	0.8-8	Not reported	0.8	Ref [39] Ref [44] Ref [45]	

PM and melting	AlSiC	3-12	69.4	1.3	Ref [38] Ref [47]	
----------------	-------	------	------	-----	----------------------	---

2.6 EFFECT OF ALLOYING ELEMENTS IN ALUMINUM

Homogeneity of metal foams and their ability to contain more gas can be enhanced by adding certain alloying elements to the parent metal Al. These additions lead, not only to the creation of a eutectic and intermetallic formation but also extend the solid solubility limit of the metal and create a wider freezing range. These intermetallic phases are also considered to be essential for foam stabilization [48]. Alloying elements affect the foaming behavior in such a way that they form stable intermetallic phases during the foaming process which increase viscosity and rigidity of cell walls. Furthermore, they not only change the melting behavior of the Al matrix, but also modify the surface tension of the alloy influencing the stability of the cell wall.

Alloying elements like Mg, Ni, Si, Zn, Fe and Cu also impart some other properties such as increased strength, hardness, and corrosion resistance [48]. A careful mixing of Mn and Ni in a correct ratio, results in the formation of intermetallics such as Al_6Mn and Al_3Ni which aid in refining the cast grain size and enable better control of recrystallization [49]. All these inclusions have an impact on foam stability in terms of their structure, distribution in the melt and their wetting behavior. Furthermore, particle size and their concentration in the melt also influence foam stability by raising the viscosity of the melt.

2.6.1 Al-Ni Intermetallics

Intermetallic compounds contain attractive properties (physical and mechanical) for multiple applications [50]. In general, intermetallic compounds show interesting features such as high melting points and good toughness due to their metallic bonding. In the case of Al-Ni intermetallic, their predominant characteristics are high thermal conductivity, low density, as well as high corrosion and oxidation resistance at elevated temperatures [51, 52]. Comparing these compounds with pure aluminum, Al-Ni intermetallics tend to have higher yield strength and compressive strength. Based on phase diagrams, six intermetallic compounds have been identified in the Al–Ni system compound: Al_3Ni , Al_3Ni_2 , Al_4Ni_3 , AlNi , Al_3Ni_5 , and AlNi_3 [53] and their formation is determined by different parameters such as composition, temperature, time, and process.

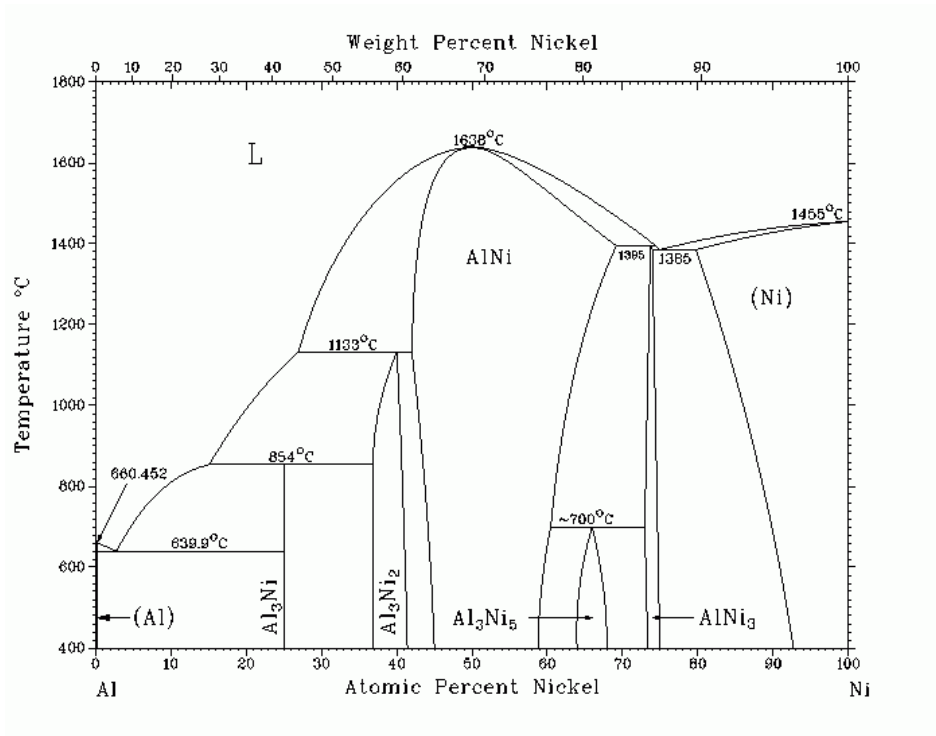


Fig. 2.9: Binary Ni–Al equilibrium phase diagram [54]

Normally, the first phase to form is always Al_3Ni , due to the large difference in interdiffusion coefficients, Ni tends to diffuse quickly into the Al instead of Al into Ni [55]. In fact, this occurrence can be clearly explained by the interfacial synergy among two thin metallic layers propose in Bené's rule. It describes that the first phase to nucleate is the phase that is closest to the low-temperature eutectic in a binary phase diagram [55]. This being the reason why Al_3Ni always forms first.

2.7 PROPERTIES OF ALUMINUM FOAMS

Aluminum foams like other metallic foams, have gained popularity due to their remarkable combination of properties, for instance: good energy absorption and acoustic damping, closed porosity, high specific stiffness, low specific weight and reasonable machinability [56]. These properties depend on their structure like size, shape, distribution of cells and especially their relative density that is determined by the ratio of foam density to the density of the solid metal [17].

2.7.1 Mechanical Properties

Metal foams have different properties compared to the solid alloys from which they are made. Mechanical properties of aluminum foams like Young's modulus, compressive strength, and flexural strength are dependent on the foam density [57]. The second defining parameter deciding the mechanical properties is the microstructure of the metallic matrix. The most important microstructural feature is the "relative density" which is the volume fraction of solid, that ranges from .03 to 0.3 [58].

2.7.1.1 Compression Behavior

The main deformation mechanisms observed in aluminum foams in relation to compression are bending and buckling of the cell walls of the foam and they are usually concentrated where density is low [59]. As compared to other metallic foams, aluminum foams when crushed, require a minimum quantity of distributed cells for its properties to fall within the bulk regime [60]. Fig. 2.10 shows a stress-strain curve for a closed cell foam subjected to an uniaxial compressive load.

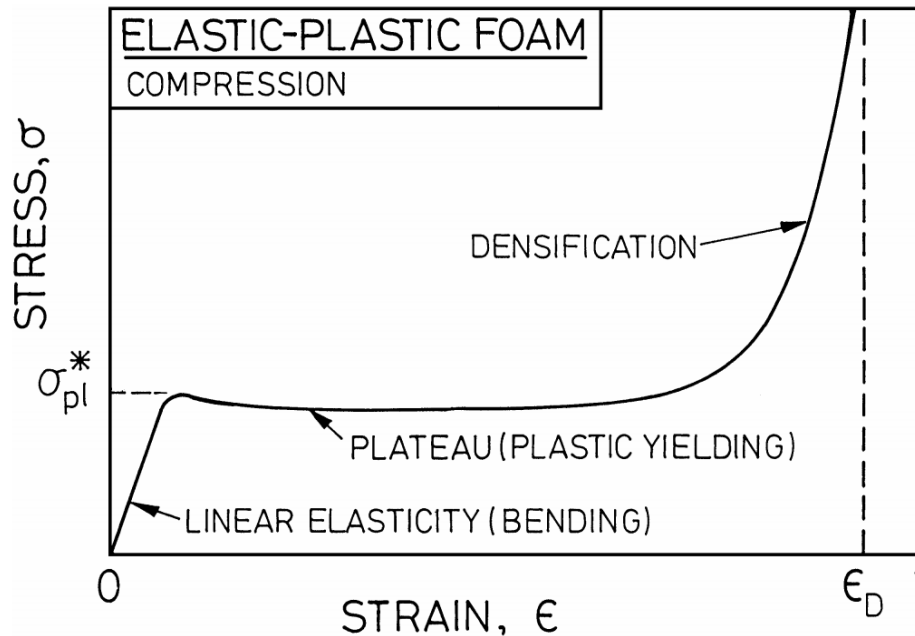


Fig. 2.10: Stress-Strain curve obtained from a uniaxial compressive load [61].

Normally the way of defining metallic foams' mechanical properties is to characterize their stress-strain performance. In terms of linear elastic behaviors, for these types of materials, it is necessary to have at least three properties: Young's modulus, E , Poisson's ratio ν and shear modulus, G .

Some foams are anisotropic (different configurations) for those more than two properties are required to establish their linear elastic behavior.

2.7.1.2 Energy Absorption

Another prominent feature of metallic foams is their ability to absorb an adequate amount of energy upon impact, without transferring the deformation pattern to the adjacent structures due to the fact that they crush upon themselves upon impact. Foams produce with metals can experience up to 70% strain at constant stress levels without reaching damaging stress values [58]. The deformation behavior can be influenced by several aspects such as foam density, cell size, cell wall thickness and alloy composition. These aspects decide whether cell walls will bend plastically, buckle or fracture [26]. The amount of energy loss in foams is about 10 times more than that of the solid metals which is the reason why they are considered attractive material choices in the automobile sector these days [17].

2.7.1.3 Three-point bending test

Several tests have been proposed for analyzing and characterizing the process of sintering in powdered metals, of which the three-point bending test is the most preferred.

For this test, porous Al samples are submitted to a constant load which is applied at midspan and two ends of the specimen on a universal mechanical tester and values of width and thickness of the specimen are measured. Yield strength, elastic modulus, and flexural strength are then calculated. The following formula is typically used to calculate flexural strength which is then used to describe failure under bending.

$$\sigma = \frac{3 F L}{2 b d^2}$$

Flexure Strength

Where σ is the flexural strength, F the maximum applied force, L the length of the span, b the width and d the depth of the sample [62].

There are several reasons for using three-point-bending for material characterization: simplicity of test procedure, suitability for cyclic and fatigue loading, the availability of simple formulas for analyzing materials, cost, convenience for fracture toughness studies and provision of subjecting the sample to tension, compression, and shear at the same time [63].

2.8 APPLICATIONS

Aluminum foams, as a result of their light weight, high stiffness to weight ratio and their excellent compression and energy absorbing behavior, have a number of applications in different industries. Their suitability for a particular application is determined by conditions such as porosity type, internal surface area, metallurgy, cost, open or closed cell, and possibility of shaping the foam. Industries like the automotive, building, biomedical, aerospace are presently focusing more and more on using these materials. Lightweight structures of Al foam have made them useful in automotive industry and in the construction of elevators [60]. Their energy absorbing quality and temperature resistance has been found useful in making fillers of crash box structures, structural parts in automobiles, parts for tail booms of helicopters and energy absorbers such as safety

equipment [64]. Some of the functional applications include heat exchangers, filtering, acoustic control, and electrochemical applications.

There are numerous other applications and uses where these porous metallic foams can be put to good use such as sandwich cores with good shear and fracture strength, packaging with high-temperature capability, flame arresters and heat shields for thermal management, electrical screeners, and biocompatible inserts.

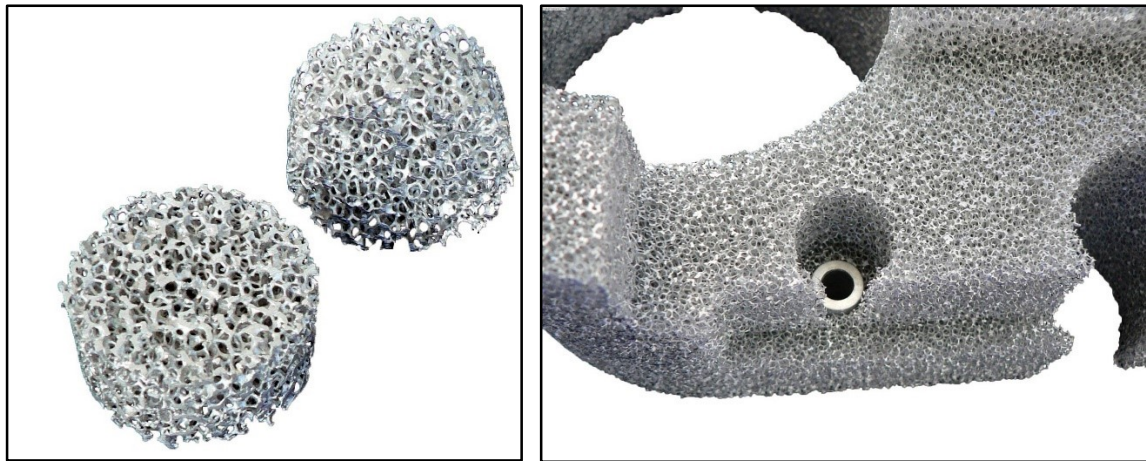


Fig. 2.11: DUACEL aluminum foam used for energy absorbers and thermal energy absorbers for medical laser applications [46]

3. OBJECTIVES

1. Assess the effectiveness of dolomite as a foaming agent for the production of aluminum foams by the powder metallurgy route.
2. Select a potential aluminum alloy that modifies the foaming properties of the metal matrix in the following manner:
 - * Increases the matrix melting point in order to eliminate the gap of temperatures with the gas release from the foaming agent.
 - * Generates a transient semi-solid phase(s) that could assist the pore formation and minimize gas loss at early stages of foaming. Promoting also the uniform nucleation of spherical pores.
3. Evaluate the compressive strength of the optimal aluminum foams produced with dolomite and compare them with values currently found in the literature.

4. EXPERIMENTAL PROCEDURE

4.1 MATERIAL SELECTION AND PREPARATION

The atomized aluminum base powder used during this study was from Alfa Aesar, with a particle size of 325 mesh and a level of purity of 99.5%. The atomized nickel powder used in the production of foams was also obtained from Alfa Aesar with a particle size of 325 mesh and a purity level of 99.7%. Dolomite, the foaming agent, was purchased in lump form from Fisher Scientific.

In order to obtain dolomite powder, a grinding procedure was performed in the laboratory. The dolomite rock was placed in a planetary ball mill (PM 200 Retsch) at 450 rev/min until an average particle size of 25 μm was achieved. The technical information about the powders is summarized below in Table 4.1.

Table 4.1: Summary of the powders used according to supplier, mesh size, level of purity and oxygen content

Element	Supplier	Size (mesh)	Purity (%)	Oxygen Content (wt%)
Aluminum	Alfa Aesar	325	99.5	0.3783
Nickel	Alfa Aesar	-325	99.7	0.366
Dolomite	Fisher Scientific	± 25	99.5	N/A

Particle size analysis was performed using a Laser Scattering Particle Size Analyzer (HORIBA LA-950) on each specific powder and the information is summarized below in Table 4.2. This step ensures that all the powder is of the desired size and distribution.

Table 4.2: Powders size analysis

Powder	Mean Size (µm)	Media Size (µm)	Std Dev (µm)	D90	D50	D10
Aluminium	16.08	16.15	99.5	21.74	16.15	10.23
Nickel	66.48	61.54	99.7	106.12	61.53	26.63
Dolomite	25.91	12.16	34.80	54.1	20.60	4.18

4.2 POWDER MIXING

In the interest of obtaining the required the mixtures for the production of foams, the following powders were mixed in different compositions and concentrations as it is shown in Table 4.3. Pure aluminum, Al-Ni alloy and the foaming agent, dolomite were added to a cylindrical plastic container with alumina balls (3:1 ball to powder ratio). The container was placed on a conventional tumbler mixer for 1 hour. Finally, powders were separated from the alumina balls using a metal grid.

Table 4.3: Mixture composition and concentration matrix

Dolomite (wt%)	Pure Aluminum	Al-5Ni	Al-10Ni	Al-15Ni
3%	X	X	X	X
5%	X	X	X	X
7%	X	X	X	X
10%	X	X	X	X

4.3 COMPACTION (Preparation of precursors)

The compaction process starts after obtaining a well-blended mixture. A required amount of the mixture was placed in a 30 mm diameter steel die previously lubricated with lithium stearate. The amount of mixture (size of the compact) was determined by applying the rule of mixtures. With this equation, it is possible to identify the necessary weight of the powder mixture that must be compressed in order to achieve a desirable volume.

$$\rho_m = \frac{x_a \rho_a}{V} + \frac{x_b \rho_b}{V} + \frac{x_c \rho_c}{V} \quad \text{Rule of mixtures}$$

where ρ_m is the theoretical density of the mixture, ρ_a , ρ_b and ρ_b are the densities and x_a , x_b and x_c are the weight fraction of the different powders.

The compaction of the powder consisted of a hydraulic uniaxial cold pressing of 556 MPa for 15 min., followed by a hot compaction of 851 MPa at 350°C for 60 min until a green dense precursor was obtained. Specifications of optimum pressures, times and temperatures are summarized in Table 4.4, classified according to chemical composition.

Table 4.4: Powder Pressing Parameters

Mixture	Sample thickness (mm)	Cold pressing pressure (MPa)	Cold pressing time (min)	Hot pressing pressure (MPa)	Hot pressing time (min)	Theoretical density (%)
Pure Al + Dolomite	15	152	15	377	45	98
Al-5-Ni + Dolomite	14.3	527	15	808	45	98
Al-10Ni + Dolomite	14	556	15	851	60	98
Al-15Ni + Dolomite	13.8	556	15	866	60	98

4.4 PRECURSORS PARTIAL-SINTERING

Prior to foaming, each precursor was subjected to a heat-treatment step in a Lindberg/Blue M box furnace for 15 and 20 min. at 450°C. This step had been added to the normal powder metallurgy procedure in order to lower the residual porosity and to obtain a partially-sintered compact.

4.5 FOAMING PROCESS

The foaming process was performed using a vertical tube furnace (expandometer) that permits the in-situ determination of the foam expansion behavior. The hot compact was inserted in a pre-heated 35 mm diameter stainless steel crucible. The interior of the crucible was previously lubricated with boron nitride. The specimen was heated between 750°C and 800°C for 19 min. The expandometer was designed with exclusive features for reading displacements of constrained foams. A lightweight piston was set on the top of the precursor, which was connected to a laser sensor that recorded the change of height caused by vertical expansion [1].

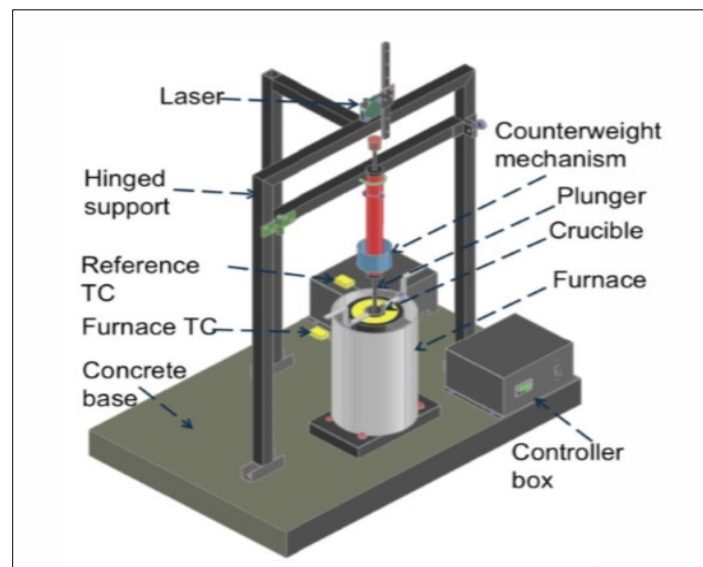


Fig. 4.1: 3D schematic of the Laser Expandometer [6]

4.6 CHARACTERIZATION OF THE FOAMS

Diverse characterization techniques were employed to study and evaluate macro and microstructure of final foams and the starting materials. SEM, ICP, and XRD were used to characterize the morphology, composition, and phases of the powders, respectively. DSC-TGA was used to determine the decomposition, weight loss and behavior of dolomite. Pore size distribution, morphology wall thickness, and other features of the foams were analyzed by 3D optical microscope. Detail description of the characterization techniques and specific settings at which they were operated can be found below.

4.6.1 Scanning Electron Microscopy (SEM)

Microstructural analysis and characterization of foamable precursors and foams were observed using scanning electron microscope (SEM-Hitachi, S-3400N). SEM was also helpful for the analysis of mixture of powders. For examination by SEM, the foaming agents in powder form were scattered onto sample holders which were coated with conductive tape on both sides. For final foam structures, samples were prepared just like those used for the optical microscopy. Elements with different atomic numbers were easily identified by SEM so no etching was required. Energy Dispersive Spectrometer (EDS--Hitachi, S-3400N) analysis was also carried out to identify the phases present in the metallic matrix of the foams.

4.6.2 X-Ray Diffraction (XRD)

To study powder composition and identify crystalline phases present, X-ray diffraction was employed using a PANalytical Xpert Pro powder X-ray diffractometer with a $\text{CuK}\alpha$ radiation at 45kV and 40mA. The x-ray diffraction patterns were obtained within an angle interval from 20 to $120^\circ 2\theta$ with a 0.02° step size. In this technique, X-rays are scattered by the atomic planes of the crystal to form X-ray spectra which give us information about crystalline nature of the material. For this purpose, crushed fine powders of foam specimens were formed and maintained in a dry environment to preserve any hygroscopic phases. X-ray diffraction study of the samples was carried out using X'Pert HighScore Plus Rietveld analysis software. Pearson's crystal database [36] was used to export the crystallographic entry to check the known phases in the Al-Ni + dolomite system.

4.6.3 Differential Scanning Calorimetry (DSC) and Thermogravimetric Analysis (TGA)

To study and characterize the decomposition of the powder mixtures and to evaluate the particle size, differential scanning calorimetry and thermogravimetric analysis (DSC & TGA- Setaram Evolution 25) were used. The scanning rate and sample mass were kept constant at $10^\circ\text{C}/\text{min}$ and 20mg, respectively. In these techniques, modifications in properties of materials (physical and chemical) are measured as a function of temperature using different DSC and DTA curves. Metal powders were placed in an alumina crucible, in the presence of a carrier gas and were subjected to various heat treatments. A microbalance was used to measure changes in mass. DSC curves were

obtained and studied with the objective of evaluating the formation of phases according to endo and exothermic reactions as it is described below.

4.6.4 3D-Optical Microscopy

For optical image analysis and to examine the morphology and microstructure of foams, a 3D optical microscope was used (Keyence-VHX-2000). This optical microscope uses visible light and a system of lenses to magnify the surface images of small samples, with a range of magnification between 0.1x to 5,000x and an observation of 360 degrees. The microscope has a motorized XYZ control, providing a depth composition function for full-focus images.

4.7 MECHANICAL TESTING

4.7.1 Compression Testing

To analyze the mechanical properties of foams, mechanical (compression) testing was performed. Cylindrical samples of the foam with parallel faces were prepared and uniaxially compressed with hydraulic compression testing rig fitted with parallel compression plates. The density of the specimen was determined by weighing the sample and measuring its external dimensions. Compression load was applied at a strain rate 1.5 and 5 mm/min and measured by using a 100 kN load cell (MTS Landmark® Testing Solutions). Strain in the foam specimen was measured by using a separate linear variable displacement transducer (LVDT). Stress-strain curves were obtained from the measured data to determine mechanical properties of Al foam.

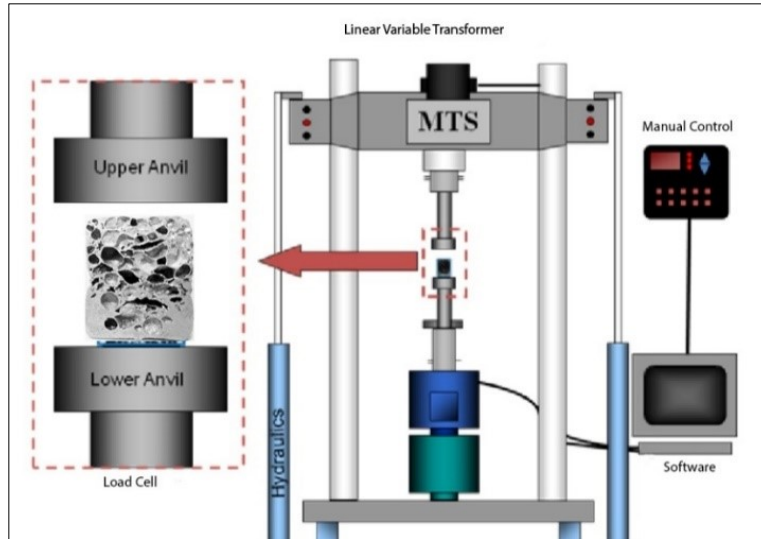


Fig. 4.2: Schematic of MTS compression machine [6]

4.7.2 Three-point bending flexural test

In order to determine the effect of the level of inter-particle bonding achieved in the precursors, three-point bending testing was used. Green dense compacts were cut and prepared in three identical pieces with dimensions of 30 mm length x 4mm thick and height of 15 mm. The specimens were placed in a three-point bending machine arranged with a span length of 25 mm between two parallel supporting pins. The tests were performed with a constant uniaxially load in an MTS (Landmark Testing Solutions) employing 100kN load and a cross head speed of 0.5mm/min. The set-up of the test can be observed in Fig 4.3.

The method provides twofold information on the degree of sintering: first, the transverse rupture strength values (TRS) give a fair indication of the level of inter-particle bonding, or partial sintering and thereafter the fracture surface examination of the specimens reveals neck formation (if any) between particles.

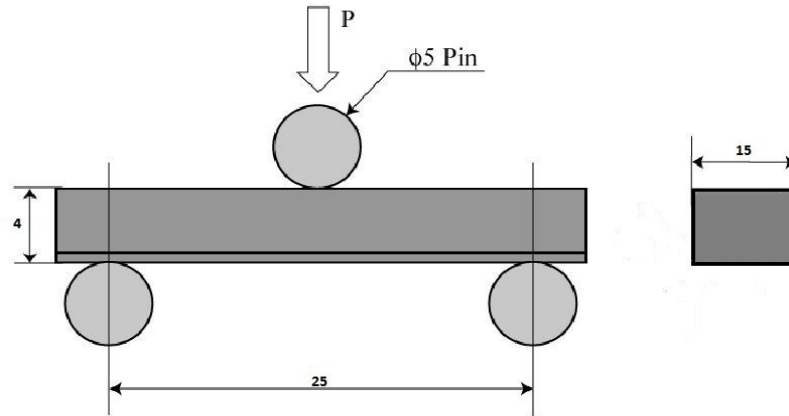


Fig. 4.3: 3-point bending test set-up for foam specimen

The following work is a journal paper being submitted to Advanced Engineering Materials and includes all the usual elements of a stand-alone article. Extended versions of the literature review and experimental procedure were described in the previous sections. The mechanical characterization of the Al-Ni foams forms a separate Chapter (6).

5. PRODUCTION OF HIGHLY POROUS AL-NI FOAMS WITH DOLOMITE AS FOAMING AGENT VIA THE POWDER METALLURGY TECHNIQUE

5.1 ABSTRACT

In this work, we successfully produced highly porous and low-cost aluminum foams via powder metallurgy route using dolomite (3-10wt %) as blowing agent. To this end, nickel additions (5-15wt %) were explored in order to reduce the temperature gap between dolomite decomposition and the melting range of the metallic matrix. We found that specific Al-Ni compositions can provide appropriate viscosities for enclosing the gas released from the decomposition of dolomite. A partial-sintering step was introduced prior to the foaming process of the compacted precursors, which resulted in high porosity levels (~85%) and volume expansion (~250%) in the final product. The partial-sintering technique was a determining key factor in obtaining highly porous cellular structures with homogeneous pore distribution.

5.2 INTRODUCTION

The ever-increasing demand for lower fuel consumption triggered in recent years the exponential research and development of light-weight materials such as aluminum foams. The metallic foams, also known as cellular or porous metals, are usually characterized by a large volume fraction of porosity sometimes reaching levels of 75 to 80%. In order to fulfill the mechanical strength, the

usually desired physical properties for such materials are large, uniform, rounded pores separated by thin continuous cell walls. The excellent deformability and strength of aluminum foams in conjunction with the high energy absorption and the ability to reduce vibration levels sometimes up to 60% make these materials outstanding candidates for crash elements in the automobile industry. Although currently aluminum foams are commercially produced on a small scale in several countries, including Canada, the elevated production costs hinder dramatically their mass production.

As found in the literature, the aluminum foams can be manufactured via different processes [1,76], however traditionally they are produced from aluminum melt precursors (i.e. “direct foaming of melts”) foamed by a gas or a blowing agent and stabilised by the addition of non-metallic particles such as ceramics (oxides, carbides, nitrides), intermetallic, fibers or fly ash. Generally, the process can be categorized according to the stabilizing particles and blowing agent. The most common blowing agents are metallic hydrides such as ZrH_2 , MgH_2 and the most widely used - titanium hydride. Although titanium hydride is the most common blowing agent due to its low decomposition temperature (450-650°C), its high price and handling hazard increase the overall manufacturing cost of Al-foams. In a sustained effort to reduce the fabrication costs of these materials, development of less expensive blowing agents constitutes the focus of the research community. Moreover, single step processes in which the blowing agents and stabilizing particles could be added simultaneously to the metallic matrix are potential candidates to further reduce production costs. In this context, the powder metallurgy (PM) route of metallic foam fabrication, alternately known as the “powder line” [77] promises these advantages.

In the specific case of aluminum foams, the powder metallurgy route (PM) has been extensively explored in our laboratory. Several studies were conducted in PM Al foam production using titanium hydride as a blowing agent [4,5] and explicit understanding of the process has been reported. In the present study, we explored the use of alternate materials such as dolomite ($(\text{CaMg}(\text{CO}_3)_2)$) as a low-cost foaming material. In addition to its attractive low price, another big advantage in using dolomite as a foaming agent is the simultaneous supply of stabilizing media. Its theoretical composition is 30.41 % CaO, 21.86% MgO and 47.73% CO_2 by mass. During the dolomite decomposition which onsets slowly and subtly ($\sim 1\text{wt}\%$) at approximately 500°C followed by a rapid ($1.77\%/ \text{min}$) and substantial release ($\sim 46\%$) between 590°C to 785°C porous oxides are formed. These oxides constitute thereafter the scaffold for foam stabilization impeding drainage of the molten metal. After a survey of the literature very limited studies have been reported on the fabrication of Al-foams using this additive [32,44,45]. The main reason could be related to the fact that while dolomite is a widely available, inexpensive mineral, the mismatch between its decomposition temperature and aluminum melting point ($\sim 660^\circ\text{C}$) limits its applicability. This mismatch is considered to be the major factor responsible for reduced foam expansion and lack of pore uniformity. One possible solution to decrease the temperature mismatch between the two components is the addition of an alloying element able to shift the melting point of the metallic matrix to the decomposition temperature of the dolomite. Such potential candidate is nickel. According to the Al-Ni phase diagram [54], nickel addition to the aluminum matrix in the range of 5 to 15wt% will trigger melting temperatures closer to the temperature range of dolomite substantial CO_2 release. The traditional PM technique of aluminum foam fabrication entails the hot ($\sim 350^\circ\text{C}$), uniaxial pressing of the powder- blowing agent mixture

into high-density compacts (>90%) [4,5] followed by heating of the compacts to the blowing agent decomposition temperature. There are several reports [79] stating that the hot pressing of the powders is rather insufficient in achieving a uniform cellular structure in the final product and they suggest additional treatments, such as extrusion, prior to the foaming step. It is said that such treatments break the tenacious oxide films encasing the metallic powders and hence good inter-particle bonding is achieved. This extra preparation step allegedly increases the final product quality. In the present study rather than using extrusion we adopted an additional step therein after referred to as the “partial-sintering” step, which is in essence an increase in the compaction temperature up to 450°C for different dwell times, and was selected to promote inter-particle bonding and hence to potentially increase the quality of the cellular structures.

The aim of the present research is to explore dolomite as a suitable foaming agent in producing low cost, highly porous aluminum foams via the powder metallurgy route. Additions of nickel as alloying elements are undertaken as a potential candidate to diminish the temperature gap between dolomite decomposition and the melting range of the metallic matrix. Finally, the effect of the partial-sintering step, in terms of volume expansion, pore structure, and foam quality is discussed.

5.3 EXPERIMENTAL

5.3.1 Precursors fabrication

Air atomized aluminum powder (99.5%, -325mesh) and nickel powder (99.7%, 325mesh); both obtained from Alfa Aesar were selected to produce the foam precursors. Four different

compositions containing 0%, 5%, 10% and 15% weight percent of Ni were prepared. Dolomite, with an average particle size of 25 μm , purchased from Fisher Scientific, was used as the foaming agent. The weight percentage of dolomite added to the Al-Ni mixtures were 3wt%, 5 wt%, 7 wt%, and 10 wt%. The morphology of the starting materials is shown in Fig. 5.1.

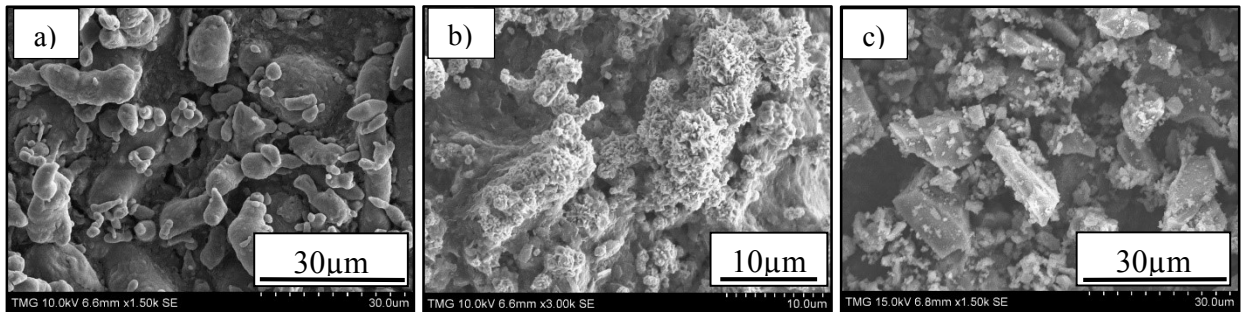


Fig. 5.1: Scanning electron microscopy (SEM) images of the starting materials: a) Aluminum, b) Nickel and c) Dolomite

The appropriate quantities of starting materials were homogenized in plastic containers with alumina balls (3:1 ball to powder ratio) on a conventional tumbler mixer for 1-hour blending time.

The homogenized powders were thereafter separated from the mixing media and compacted in 30 mm diameter steel dies previously lubricated with lithium stearate, and cold uniaxial pressed at 556MPa for 15min. This was then followed by warm compaction at 350°C for 60 min with an applied pressure of 851 MPa until 98% of theoretical density was obtained for each sample. The specimens were thereafter subjected to an additional partial-sintering step. The partial-sintering procedure entailed sample pre-heating at 450°C for 15 min in a Lindberg box furnace. This approach resulted in an increase in samples density close to the theoretical range. In order to evaluate the influence of the partial-sintering step on foam evolution, some of the specimens were

retained in the “as-compacted” condition with no additional partial-sintering. These samples were thereafter foamed in similar conditions as the partially-sintered specimens and the obtained results were compared.

5.3.2 Foaming procedure

The “as-compacted” and “partially-sintered” specimens were placed in a pre-heated 35mm diameter steel crucible previously lubricated with boron nitride. The crucible-precursor assembly was thereafter suspended inside a vertical tube furnace (expandometer) at 750°C - 800°C for 16 min. The expandometer was designed with the exclusive feature, which enabled in-situ laser measurement of the expanding foam. Additional details of the equipment are provided elsewhere [65].

5.3.3 Characterisation techniques

Several characterization techniques were employed to analyze and evaluate the micro and macrostructural features of the starting materials, precursors and the obtained foams (metallic foams). A scanning electron microscope (SEM, Hitachi – S4300N) equipped with Energy-dispersive X-ray spectroscopy (EDS) was used to characterize the morphology of starting materials and cell structures of the foams. Phase determination was performed with X-ray powder diffraction (XRD; X’Pert Pro-PANalytical) and confirmed thereafter via EDS. Thermogravimetric analysis (TGA) and Differential Scanning Calorimetry (DSC; Setaram Evolution-24) was used to determine the decomposition behavior of dolomite. Foams cross-sections and pore size distribution were analyzed via 3D optical microscopy (Keyence-VHX-2000). Three-point bending was employed to evaluate the degree of partial-sintering of the precursors. The test was performed with

an (MTS Landmark® Testing Solutions). The resulting fractures surfaces of the partially-sintered precursors were analyzed via SEM and EDS.

5.4 RESULTS

5.4.1 Optimum concentration of additives

All the results depicted in this section were obtained with partially-sintered specimens as previously described in the experimental section. One of the goals of the present research was to determine the optimum combination of dolomite and nickel additions to aluminum base metal in order to obtain the best possible combination of volume expansion, porosity and homogeneous pore structure in the final product. To this end, a design of experiments matrix in which both the nickel content and dolomite percentage were varied was undertaken. The results obtained in terms of porosity values and volume expansion of the foams are presented in Fig. 5.2 a) and b), respectively. As observed in Fig. 5.2, an increase in dolomite content from 3wt% to 7wt% generated, as expected, an increase in both porosity and volume expansion of the foams for all the compositions studied. It appears, however, that a further increase in dolomite content to 10wt% results in a decrease of these values for all compositions studied. It should also be noted that the highest contribution to foam porosity and volume expansion is triggered by the increase of nickel content that appears to saturate at around 10wt%. Based on these findings, the ideal combination of additives which results in the highest porosity levels (~ 86%) and volume expansion (~244%) of the foams is 10wt % Ni (Al-10Ni) with 7wt% dolomite as a foaming agent.

Another aspect of utmost importance in metallic foams is the homogeneity of the pore structure. The cross-sectional features of the above-described foams are shown in Fig. 5.3. Due to the similarities between pure Al and Al-5Ni samples, these were omitted. As clearly observed in Fig. 5.3, the highest porosity levels are recorded by the 7wt% dolomite containing precursors with elevated Ni contents (10 and 15wt%) further confirming the results shown in Fig. 5.2 a).

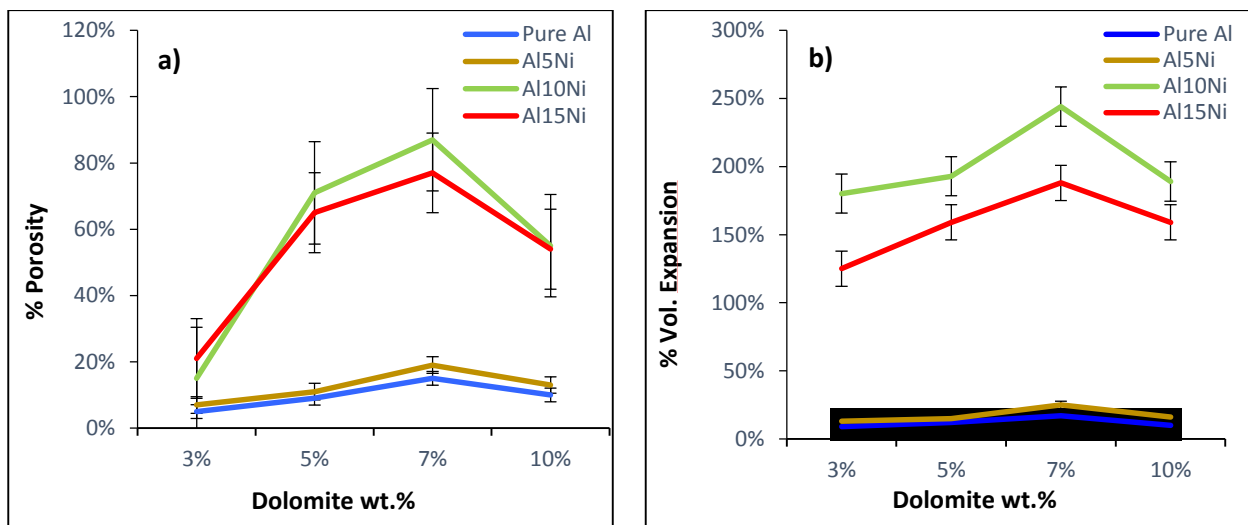


Fig. 5.2: Porosity levels (a) and volume expansion (b) of cellular specimens produced from precursors containing 0wt% Ni (pure Al), 5wt% Ni (Al-5Ni), 10wt% Ni (Al-10Ni) and 15wt% Ni (Al-15Ni) with increasing dolomite content of 3, 5, 7 and 10wt%

Although both samples (10 and 15wt% Ni) present a homogeneous pore structure the sample containing 15Ni % (Al-15Ni – 7wt% dolomite) shows a rather poor foaming at the base of the specimens. According to these results, it can therefore be stated that among all the systems studied here, the cellular material obtained from a precursor containing 10wt% Ni (Al-10Ni) and 7wt%

dolomite exhibits the optimum combination of foam porosity, volume expansion, and homogeneous cell structure.

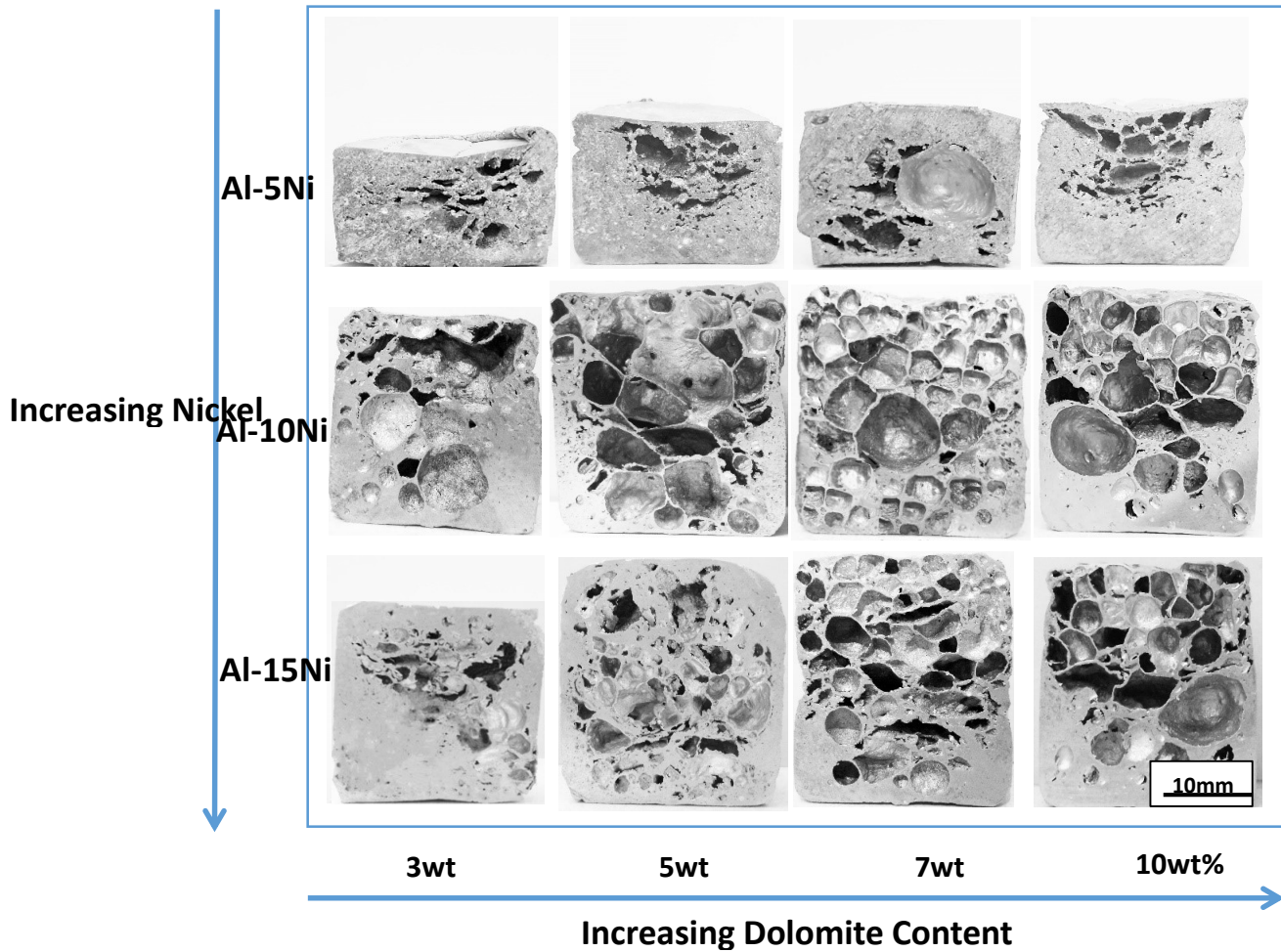


Fig. 5.3: Macrostructure of the resulting foams obtained from partially-sintered precursors of various dolomite and nickel contents

5.4.2 Foaming behavior of the partially-sintered precursors

In order to establish the influence of the partial-sintering step on the foaming process, two sets of precursors in “as-compacted” and “partially-sintered” state were evaluated. The typical foaming

behavior of the compacts in terms of volume expansion as well as the temperature evolution as a function of the foaming time is presented in Fig. 5.4. As it can be easily observed, the “as-compacted” precursors containing 15wt%Ni (Al-15Ni) with 7wt% dolomite, exhibit a limited volume expansion of approximately 20% whereas high levels of expansion of approximately 160% (i.e. 8 times greater) are recorded for the “partially-sintered” precursors of identical composition. Moreover, the “partially-sintered” precursors showed two distinct expansion steps following intimately the dolomite two-stage decomposition as determined from DSC analysis (appendix A) and that is generally agreed upon [80,91].

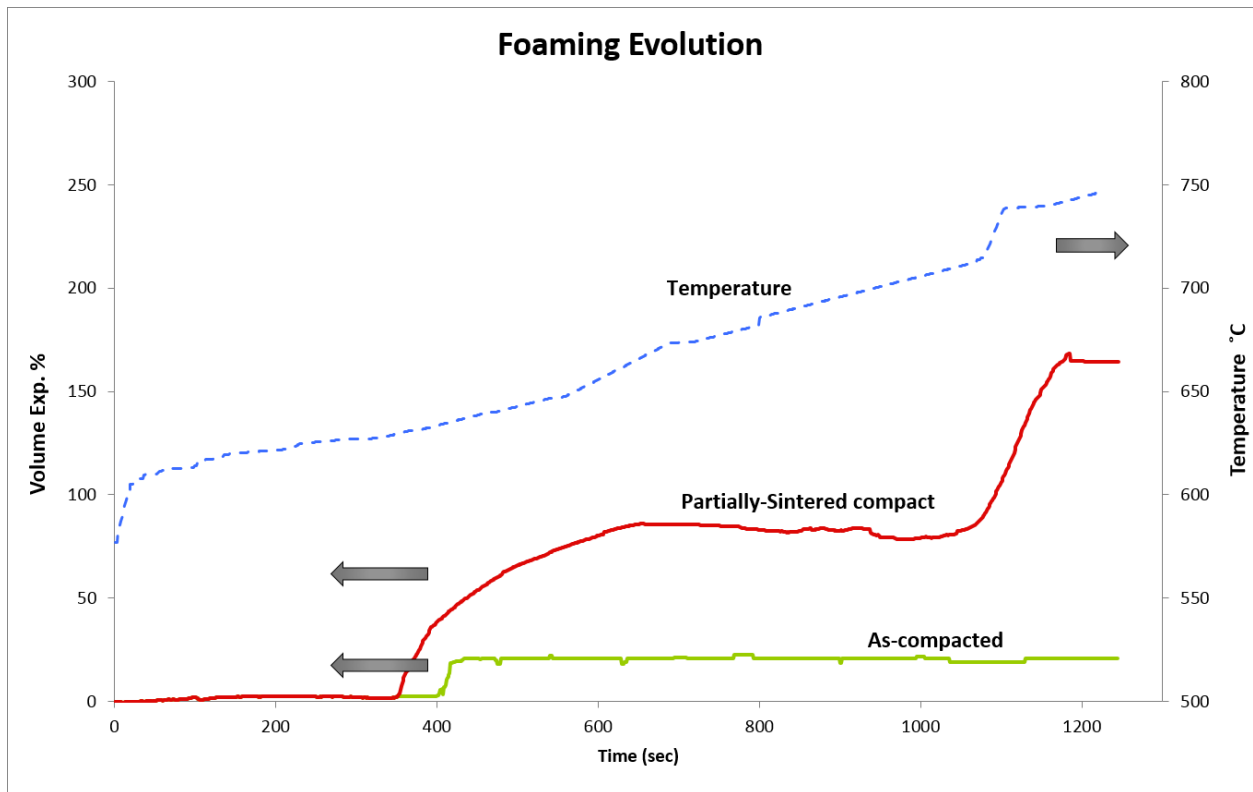


Fig. 5.4: Comparison of foaming evolution of Al-15Ni with 7wt% dolomite precursor in the “as-compacted” vs partially-sintered state

5.5 DISCUSSION

5.5.1 Foaming mechanism

The foaming process which employs Al-Ni high-density compacts with dolomite as foaming agent experiences three main evolution stages. Initially, with the temperature increased, the particles mobility also increases and neck growth begins to develop. The pore nucleation starts to form (in the shape of cracks) at the first phase of decomposition of dolomite (MgCO_3) (at around 600°C - 650°C) while the partially-sintered precursor is still solid (state 1). In the second stage, the partially-sintered precursor reaches higher temperature (650 - 700°C) melting commences and becomes a two-phase region ($\text{L}+\text{Al}_3\text{Ni}$) while MgCO_3 continues decomposing (stage 2). When the pore channels have sufficiently developed, controlled pore growth occurs. Finally, after a significant period of time, with the continuous increase in temperature, more CO_2 evolved during the second phase of dolomite decomposition (CaCO_3), and results in further pore growth. At temperatures above 700°C CaCO_3 releases CO_2 and the pores become more spherical until a highly porous, expanded structure is formed (stage3). Fig. 5.5 schematically illustrates this foaming process and evolution for a partially- sintered Al-10Ni precursor.

However, during the current study, “as-compacted” precursors despite the high level of theoretical density achieved in the green state did not manifest this behavior. The released gases caused the “as-compacted” precursors to initially expand slightly but after a short period of time, no additional dimensional change was recorded as depicted in Fig. 5.4.

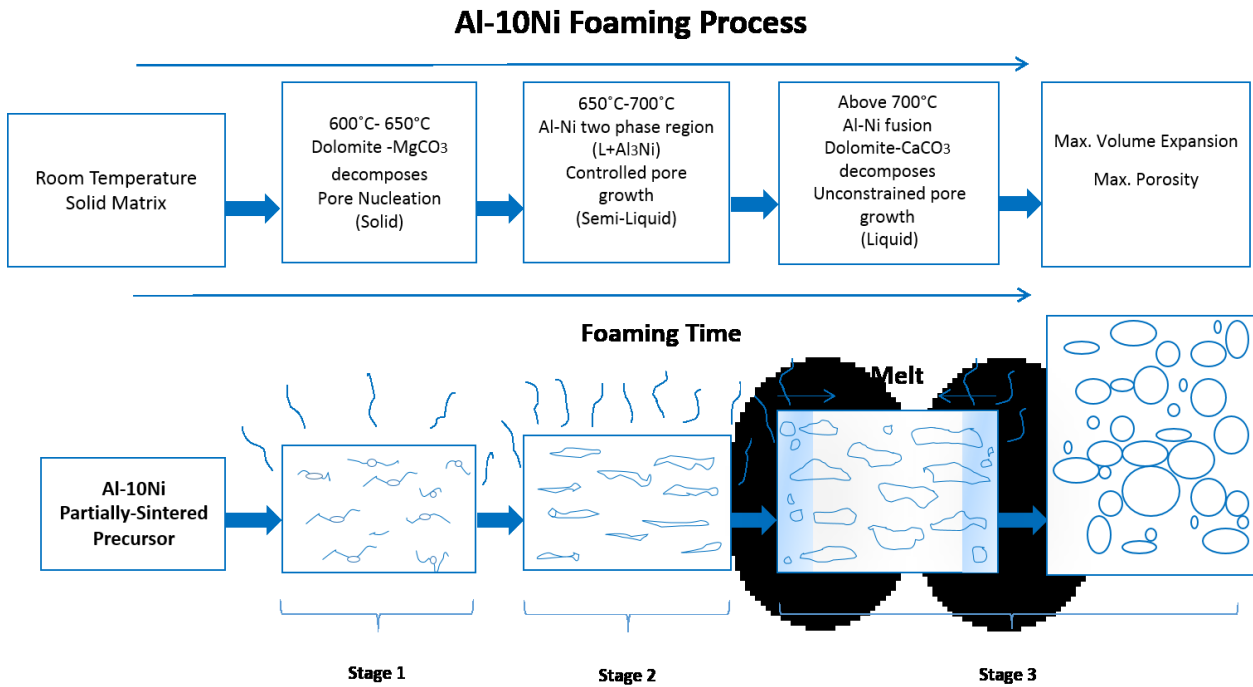
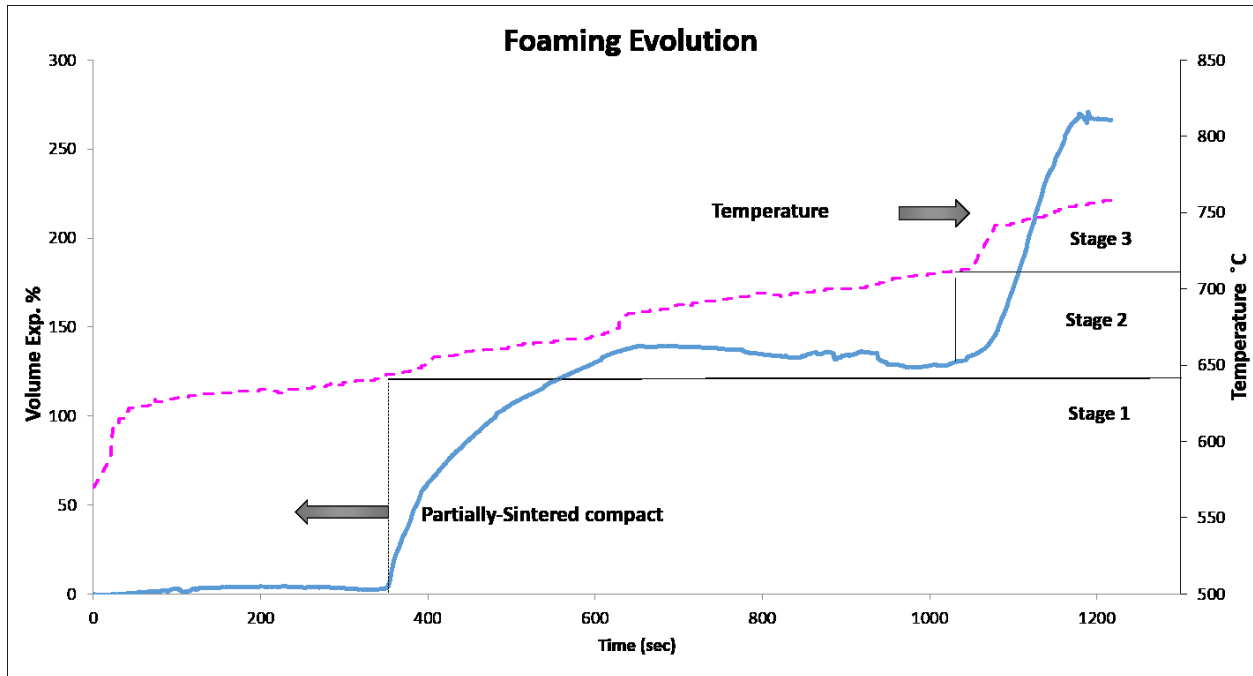


Fig. 5.5: Schematic representation of the foaming process and evolution of Al-10Ni foam.

5.5.2 Influence of the Partial-Sintering step on foam evolution

In the current investigation, it was observed that the partial-sintering step plays an important role in the foaming process, as clearly illustrated in Fig.5.4. Foams exhibiting 8 to 12 times greater volume expansion were obtained when the precursors underwent partial-sintering step of the despite the high density (>97% of the theoretical density) of both “as-compacted” and “partially-sintered” specimens.

The mechanism that governs this behavior is believed to be related to the level of inter-particle bonding developed in the precursors. In order to determine the influence of this parameter, three-point bending testing was used. The method provides twofold information on the degree of sintering: first, the transverse rupture strength values (TRS) give a fair indication of the level of inter-particle bonding, or partial sintering and thereafter the fracture surface examination of the specimens reveals neck formation (if any) between particles. The bend test specimens were prepared from “partially-sintered” precursors at 450°C for two different dwell times of 15 and 20 min respectively. Test bars originating from “as-compacted” samples were also produced. Details revealing the testing conditions, TRS values as well as the resulting volume expansion and porosity level of the final foams containing 10wt%Ni and 7wt% dolomite are presented in Table 5.1. Fracture surfaces resulting from the test bars are presented in Fig. 5.6.

As observed from Table 5.1 the “as-compacted” specimens showed TRS values of 58MPa whereas partially-sintered specimens treated at 450°C for 15 and 20 min showed greater than double values of 123MPa and 157MPa, respectively.

Table 5.1: TRS data of Al-10Ni with 7wt% dolomite precursor in the “as-compacted” and partially-sintered state

PARTIAL-SINTERING CONDITIONS					
Al-10Ni + 7wt% Dolomite	Temperature (°C)	Time (Min)	TRS Strength (MPa)	Average Vol. Expansion (%)	Average Porosity (%)
“as-compacted”	N/A		58	30	6
Partially-sintered I	450	15	123	244	77
Partially-sintered II	450	20	157	243	70

This indicates that the partial-sintering treatment has promoted inter-particle bonding to develop through partial sintering via both volume diffusion and grain boundary diffusion [82]. In fact, by examining the fracture surfaces of the resulting test bars (Fig. 5.6) it can be clearly seen that distinctive failure modes can be identified in the three specimens tested. As seen in Fig. 5.6 a) and at higher magnification shown in Fig. 5.6 b), the “as-compacted” specimens present a high degree of particle packing which is consistent with their high green density but the material remains confined to the original, individual particles which present non-existent sintering or interconnectivity.

Alternately, for the partially-sintered specimens after both dwell times shown in Fig. 5.6 c) to f), the inter-particle bonds are evident on each particle, resulting in the increase in strength when compared with the as compacted specimens. The partially-sintered specimens show a mixed ductile-brittle fracture mode, intrinsic to their chemical composition; the fracture is a combination of ductile dimples and intergranular brittle zones clearly illustrating the well-developed inter-particle partial sintering. This well-developed particle connectivity in turn influences the volume expansion and porosity of the resulting foams.

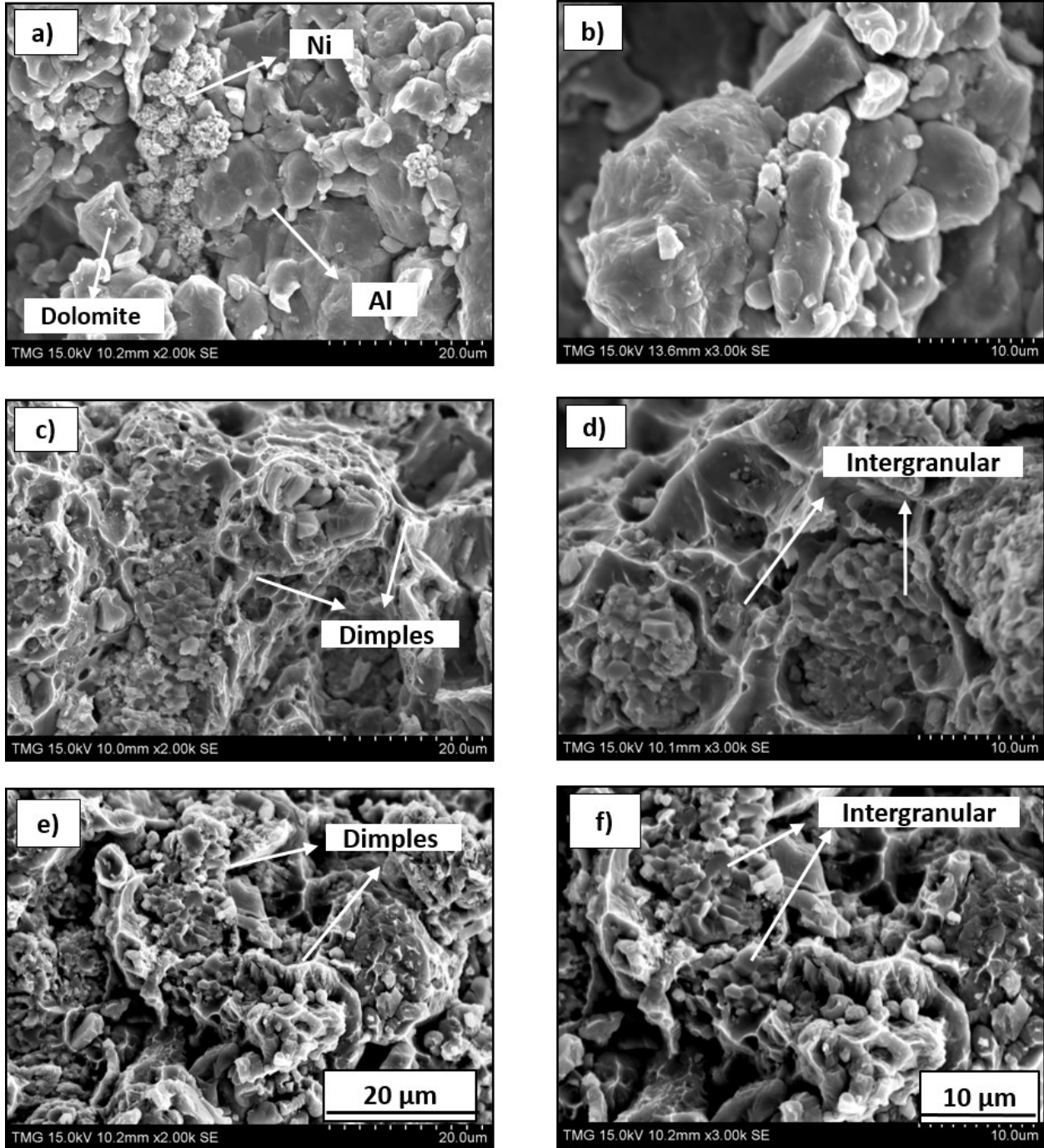


Fig. 5.6: Fracture Surfaces of Al10Ni with 7wt% compacts with 98% of the theoretical density: “as-compacted” (a and b-higher magnification); Partially-sintered I at 450°C, 15 min (c and d – higher magnification) Partially-sintered II at 450°C, 20 min (e and f – higher magnification)

By examining the results shown in Table 5.1, it appears that for the present system there is an ideal level of particles interconnectivity in the precursor which triggers an optimum foam expansion. For instance, the partially-sintered specimens heat-treated for longer times i.e. 20 min (Partially-sintered II) show the highest TRS values. However, the resulting foams from both precursors were comparable in terms of volume expansion and porosity (Table 5.1). By examining in detail the fracture surfaces of the test bars it can be noted that while both specimens presented relatively similar characteristics, in the Partially-sintered I samples (Fig. 5.6 d)) the existence of ductility dimples is easily observed whereas in Partially-sintered II specimens (Fig. 5.6 f)) the brittle mode showing intergranular fracture is more obvious. EDS analysis (appendix B) revealed that the ductility dimples were aluminum rich areas whereas the cluster of particles exhibiting intergranular fracture were in essence Al-Ni rich corresponding to initial Al_3Ni formation. It is therefore believed that the formation of dimples was mostly caused by aluminum neck growth and diffusion of grain boundaries between aluminum particles. Whereas the brittle zones were the result of the incipient formation of Al_3Ni intermetallic during partial-sintering. Longer exposure times (i.e. 20 min) at high temperature would trigger an increase in intermetallic formation with a corresponding decrease of the ductility dimples. This in turn appears to influence the amount of CO_2 retention and, although a stronger inter-particle connectivity is obtained due to embrittlement no subsequent improvement in foaming characteristics was achieved. Therefore, for the current study, using the present experimental conditions the optimum partial-sintering treatment was 450°C for 15 min (Partially-sintered I).

5.5.3 Influence of Nickel and Dolomite additions on the foaming process

5.5.3.1 Influence of Nickel additions

Another important parameter influencing the foaming behavior of the aluminum matrix with dolomite as a blowing agent was the addition of nickel. According to the literature [83] higher porosity levels can be achieved in Al foams by alloying or by incorporating reinforcement particles. Based on this principle, Ni additions of 5, 10 and 15wt% were examined. As previously seen in Fig. 5.2 a) and b) and explicitly in Fig. 5.3, foams obtained from compositions containing 5wt%Ni (Al-5Ni) showed the lowest porosity and volume expansion. The reason behind this behavior is related to the fact that according to the Al-Ni phase diagram [78], Al-5Ni is a eutectic composition which melts at 640°C. Therefore, at the temperature at which CO₂ is released, the metallic matrix is fully liquid and, hence, for the present composition any gas retention imposed by the partial-sintering step ends once the eutectic temperature is reached. As a consequence, the bubbles produced from dolomite decomposition are free to outflow and escape to the surface. A similar scenario is also observed for foams produced from pure Al. Akin to the eutectic Al-5Ni, pure Al also melts a unique temperature, which albeit higher and closer to the first CO₂ release, is unable to retain the foaming gas. These results clearly illustrate that in order for metallic foams to be successfully produced via the PM method, an increase in melt viscosity is necessary. This is usually achieved by the incorporation of at least one solid phase in the melt [84]. As such, higher Ni containing compositions, i.e. Al-10Ni and Al-15Ni exactly meet this requirement. For both these compositions, melting begins at the eutectic temperature and occurs over a range of temperatures, i.e. between 640°C and 710°C for Al-10Ni and between 640°C and 780°C for Al-

15Ni. Above the eutectic temperature, within their respective melting ranges, both these compositions present two phases: liquid and Al₃Ni crystals (L+Al₃Ni). With an increase in temperature to 650°C (i.e. the first dolomite decomposition peak), the mass fraction of solid in Al-10Ni is approximately 0.1. Consequently, a reasonably high viscosity liquid phase exists in the melt (mushy zone) which limited CO₂ release during the initial decomposition of dolomite (stage 2). At the second CO₂ release which commences at around 710°C, the system approaches the liquidus line, only a little solid Al₃Ni remains, but is sufficient to maintain, along with the oxide particles formed after dolomite decomposition, a higher viscosity for prolonged bubble retention.

For compositions containing 15wt % of Ni (Al-15Ni) the mass fraction of the solid in the melt at 650°C is approximately 0.25, i.e. 2.5 times higher than Al-10Ni and at 710°C is about 0.15. This high amount of solid in the melt hinders the uniform distribution and dispersion of the blowing gas which eventually agglomerates heterogeneously into bigger clusters, preferentially at the top of the foams and therefore less homogenous porosity and consequently reduced volume expansion is observed in these foams (Fig. 5.4). For instance, for compositions containing 7wt% dolomite the 15wt% Ni additions resulted in foams exhibiting 1.5 times lower volume expansion than foams obtained from 10wt% Ni additions. It can, therefore be observed that the best composition to render the maximum volume expansion and uniform distribution of pores is Al-10Ni, which is ultimately related to achieving an adequate viscosity in the melt.

5.5.3.2 Influence of Dolomite Content

In order to determine the optimum foaming agent content which will result in a maximum volume expansion and uniform distribution of pores, precursors containing 3, 5, 7 and 10wt% dolomite

were prepared, as previously explained. The results indicate, as depicted in Fig.5.2, that an increase in the dolomite content triggers an increase in both porosity levels and volume expansion up to a concentration of 7wt% dolomite for all compositions studied. A further increase of blowing agent content to 10wt% results, however, with a slight decrease of expansion. Theoretically, the amount of gas released is higher when 10wt% dolomite is used, 2.9×10^{-2} moles of CO_2 compare to the 2.0×10^{-2} moles resulted from 7wt% dolomite. Whereas, there is a decrease in porosity from 80% to 60% and a corresponding decrease in volume expansion from 250 to 170%. This fact is not surprising considering that for a given melt viscosity the amount of gas that could be efficiently retained and properly dispersed during the foaming process is usually the same. Conversely, the more gas released, the higher probability that the gas bubbles will coalesce and hence a less uniform porous structure would be achieved; a fact clearly observed in Fig. 5.3, foams Al-10Ni with 10wt% dolomite. This finding is in agreement with the study conducted by Barnhart et al. [83,29] which demonstrated that there is a precise content of foaming agent above which the maximum expansion obtained becomes independent. In the present study, the optimum dolomite content was found to be 7wt% above which a further increase triggered a slight decline in foams expansion and growth.

5.5.3.3 Pore Morphology, Microstructure and Phase analysis

Fig. 5.7 shows the pore cell structures of foams obtained from “partially-sintered” precursors containing the optimal dolomite content (7wt %) but different nickel additions.

The multiple defects of Al-5Ni showed in both the macrostructure (Fig. 5.7 a) and b)) and pore surface microstructures (Fig. 5.7 c) insufficient pore formation and variability in the cell structure

of this eutectic composition are attributed to the gravity-driven drainage in the liquid phase of reduced viscosity, as previously explained.

On the other hand, foams obtained from high Ni compositions (Al-15Ni – Fig. 5.7 g) to i)) which contain a relatively high fraction of solid material throughout the foaming process, present large pores of different sizes and shapes heterogeneously distributed within the sample. Moreover, an inconsistent variance in the wall thickness and wall rupture as clearly seen in Fig. 5.7 g) and h). It is believed that the high viscosity of the liquid phase prevents a uniform dispersion of the evolving gas which creates an inconsistency in pore formation caused by coarsening bubbles. Classic pore coalescence occurred by an exchange of gas between bubbles through the thin walls creating a constant rupture of cell walls. The high pressure on the cell surface as illustrated by the roughness of the internal surface of the pores (Fig. 5.7 i)).

Foams with a moderate Ni content (Al-10Ni – Fig. 5.7 d) to f)), which resulted from precursors containing optimum viscosity levels in the liquid during the foaming process, exhibited well developed homogeneous pores distributed with relatively spherical shape and consistent cell walls thickness as predominant characteristics. The average pore size was 3 mm in diameter, which is almost three times larger than the size of pores reported in the literature and obtained with the same foaming agent [35,38,39,41,43,47,]. The wall thickness was approximately 0.23 mm. It appears that for this particular composition, the optimal viscosity in the liquid was achieved during stage 2 of expansion (Fig. 5.5). Magnesium carbonate further decomposes during stage 2 and small cells grew following nucleation (stage 1) while the alloy remains as two-phases (L+ Al₃Ni).

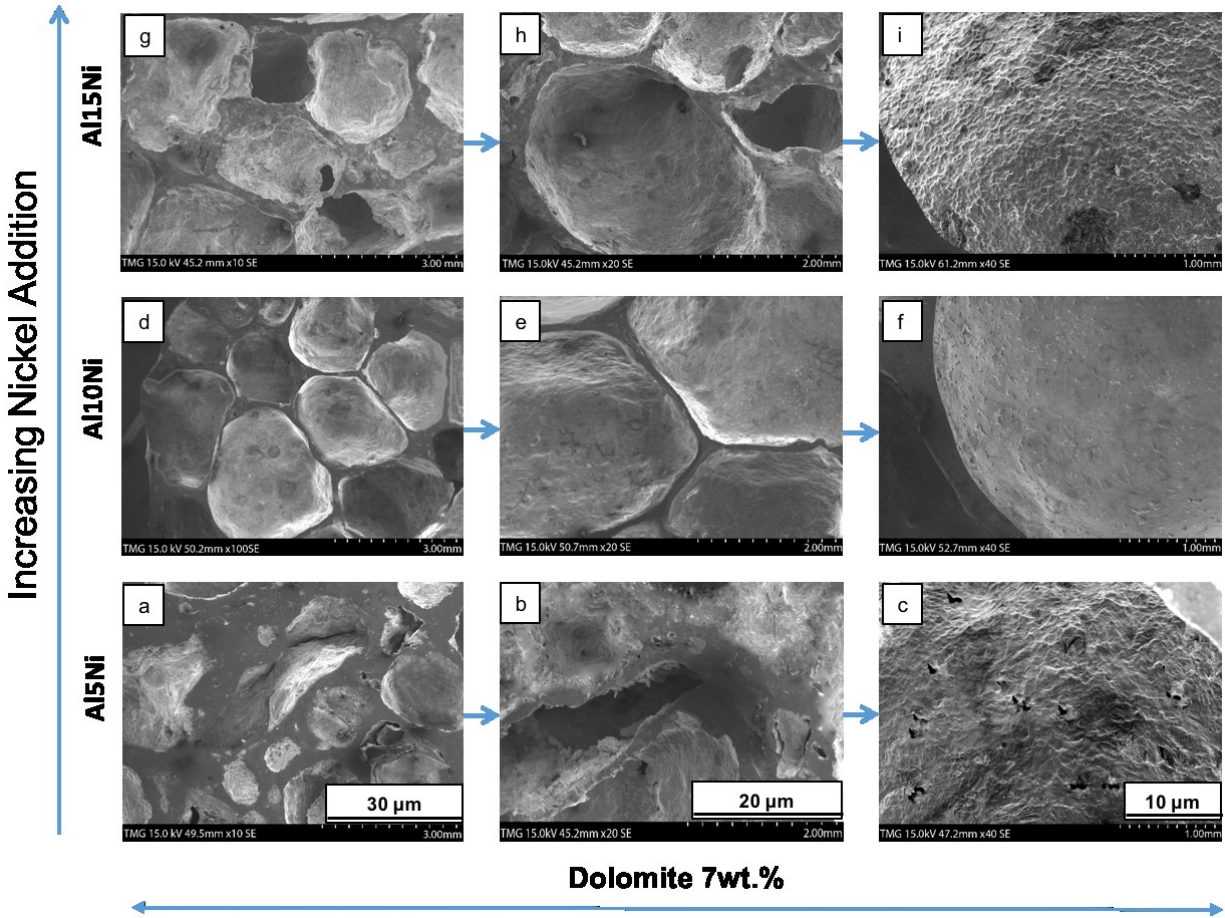


Fig. 5.7: Pore morphology for foams obtained from precursors containing 5wt%Ni (Al-5Ni); 10wt%Ni (Al-10Ni) and 15wt% Ni (Al-15Ni) with 7wt% dolomite

During stage 3 when a higher temperature is reached and only a small amount of solid phase existed in the melt, calcium carbonate started to decompose and larger cells grew [39,47]. A constant rate of gas release enhanced steady growth of pores avoiding coalescence and coarsening of bubbles due to the higher viscosity of the alloy matrix which also contained oxide particles. The matrix allows the development of well-formed pores which are defined by their roundness, smooth surface, absence of defects (Fig. 5.7 f) and well-defined plateau borders.

Another factor that contributes to the morphology of the pores is the presence of Al_3Ni particles in these foams. It is considered as an additional driving force that contributes to the geometry and distribution of the cells. Al_3Ni particles reduce the free energy in the melt by creating a solid-solid interface during the sintering process [66]. The presence of the intermetallic phase Al_3Ni in the final cellular material (Al-10Ni) was investigated via EDS and XRD analyses (Appendix D).

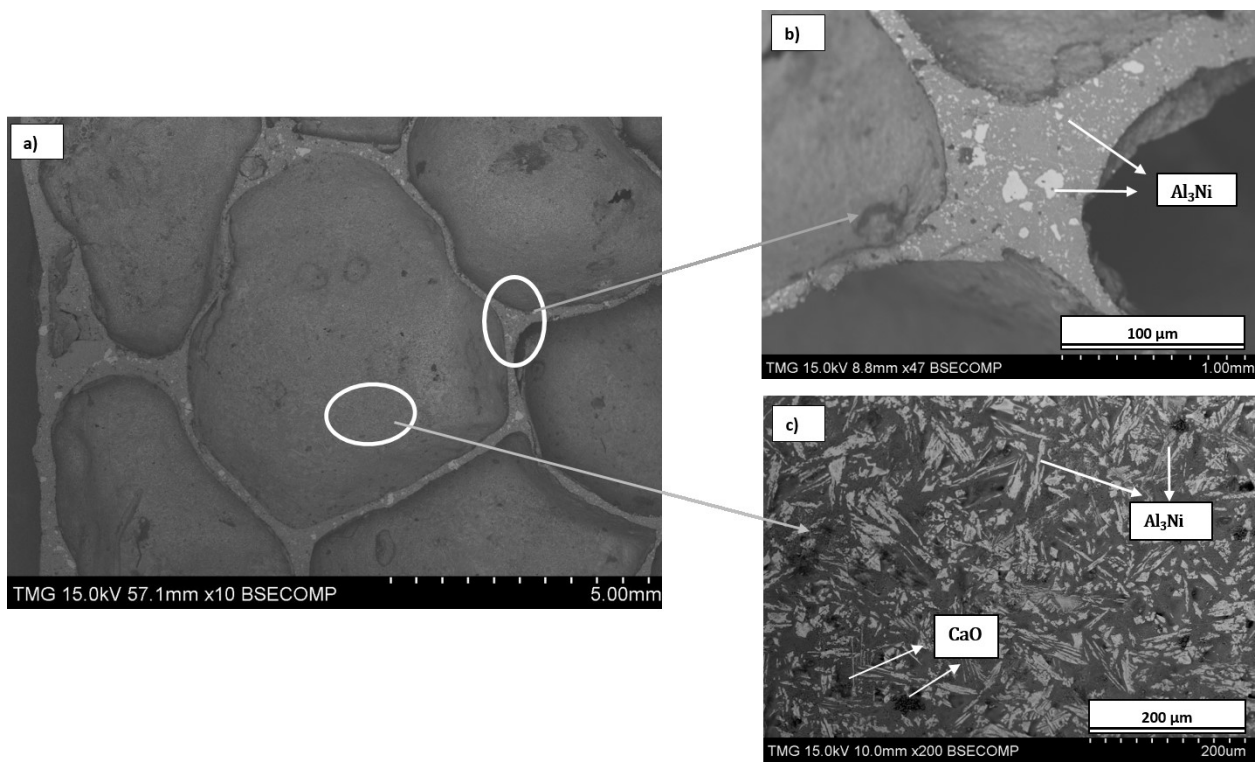


Fig. 5.8: Microstructure of Al-10Ni Foam with 7wt% (a) Pore morphology, (b) Plateau Border zones and (c) Internal cell surface

SEM images of the foam plateau border and the internal cell surface are shown in Fig. 5.8. As observed in Fig. 5.8 b) the cell walls are generally curved with a thickness ranging between 0.15

and 0.26 mm. It can be observed that the precipitation of Al_3Ni is arbitrarily spread within the cellular material and it was found in both the cell wall cross-section (Fig. 5.8 b)) as well as on the internal cell surface (Fig. 5.8 c)). A higher magnification of the pores revealed a smooth internal cell surface and, as identified by EDS analyses, it was discovered the presence of oxides. The existence of these solid particles is not detrimental to the foaming process, considering that solid particles obtained during decomposition of dolomite such as MgO and CaO and even incompletely dissociated carbonates, provide melt stabilisation by reducing the surface tension in the cell walls [43] and still contributing to the melt viscosity once all the Al_3Ni has dissolved.

5.6 CONCLUSIONS

To the best knowledge of the authors, the fabrication of foams with dolomite as foaming agent and nickel as additive was undertaken and successfully demonstrated here for the first time. This study reveals that dolomite can be an effective, alternative foaming agent to the currently used hydrides providing that its two decomposition stages are matched by a sufficiently viscous liquid phase during the foaming step. The partial-sintering step introduced here prior to foaming offered a strong inter-particle bonding in the precursors and hence a longer CO_2 retention which in turn resulted in elevated volume expansions and highly porous structures that followed intimately the dolomite decomposition stages. The most efficient partial-sintering treatment was found to be at 450°C for 15 min (Partially-sintered I).

The optimum combination of additives was found to be 7wt% dolomite and 10wt% Ni. This resulted in specimens exhibiting approximately 250% volume expansion and 86% porosity. The

cellular foam obtained showed well-developed pores, homogeneously distributed and with relatively spherical shape and consistent cell walls thickness. The average pore size was 3 mm in diameter, which is almost three times larger than the size of pores reported in the literature obtained with this foaming agent.

Furthermore, within the foaming process intermetallics (Al_3Ni) resulting from Ni additions and oxides such as MgO and CaO were formed which are known to be beneficial to foam stabilization.

As demonstrated, the highly porous structures obtained in the present study were the result of: (i) a partial-sintering protocol; (ii) a selection of the appropriate mass of foaming agent which released the optimum amount of CO_2 and (iii) an adequate nickel addition that renders optimum viscosity in the liquid (mushy zone) to efficiently encapsulate, control and distribute the blowing gas throughout the foaming stage.

6. MECHANICAL CHARACTERIZATION OF AL-NI FOAMS

6.1 Compression Test

To analyze the mechanical properties of Al-Ni foam, compression testing was performed. Cylindrical samples of the foam with parallel faces were prepared and uniaxially compressed using a hydraulic compression testing rig fitted with parallel compression plates. The density of the specimen was determined by weighing the sample and measuring its external dimensions. Compression load was applied at a strain rate 1.5 mm/min and measured with a 100 kN load cell. Strain in the foam specimen was measured by using a separate linear variable displacement transducer (LVDT). Stress-strain curves were obtained by measured data processing which was then used to obtain the compression properties of Al-Ni foam.

In order to determine the stress-strain behavior of Al-Ni foams and compare the results with the previous studies of aluminum foams using dolomite, specimens prepared with the optimum conditions discussed in the previous sections were produced and machined. The objective of machining was to obtain uniform cylinders without a thick external skin, as it is shown in Fig. 6.1.

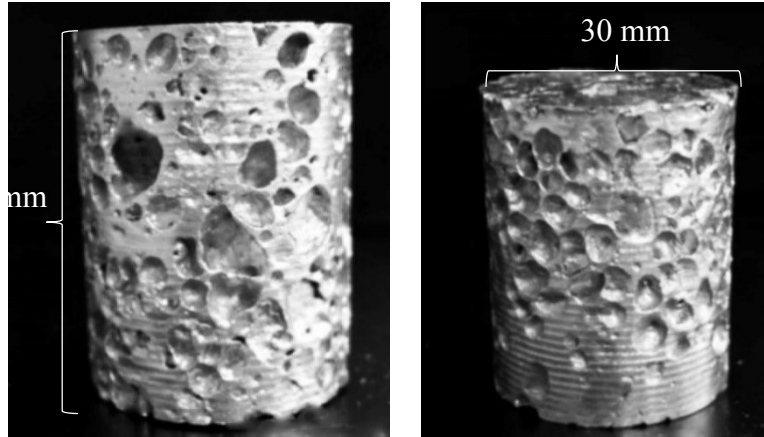


Fig. 6.1: Machined specimens at the maximum level of expansion of Al-10Ni 7 wt.% Dolomite

The final dimensions of the foams were 40 mm in height and 30 mm in diameter. To perform a conventional compression test on the foams, a size of ratio of $d/h=0.5$ in the specimens was chosen to counterbalance buckling and barreling effects during the test. The uniaxial force at 1.5 mm/min was recorded versus the change of dimension of the foam. Fig. 2.10 in Chapter 2 illustrates typical ductile behavior as expected from a metallic foam or a porous energy absorber. The compressive deformation that the samples experienced generated smooth stress-strain curves. The initial stage of this compressive deformation is a linear elastic response to the edge bending and face stretching [82]. While the stress in the foam increases, the internal cells experience progressive damage caused by three factors: elastic buckling, yielding and fracture, this stage is called “plateau” [58]. After this stage, an exponential increase in slope of the curve occurs, which is attributed to damage and crushing of the cells. This stage is known as densification.

Fig. 6.1 shows the typical test sample prepared for compressive testing and the stress-strain behaviour of foams for Al-10Ni and Al-15Ni compositions prepared with 7 and 10wt% dolomite.

The obtained results are shown in Table 6.1.

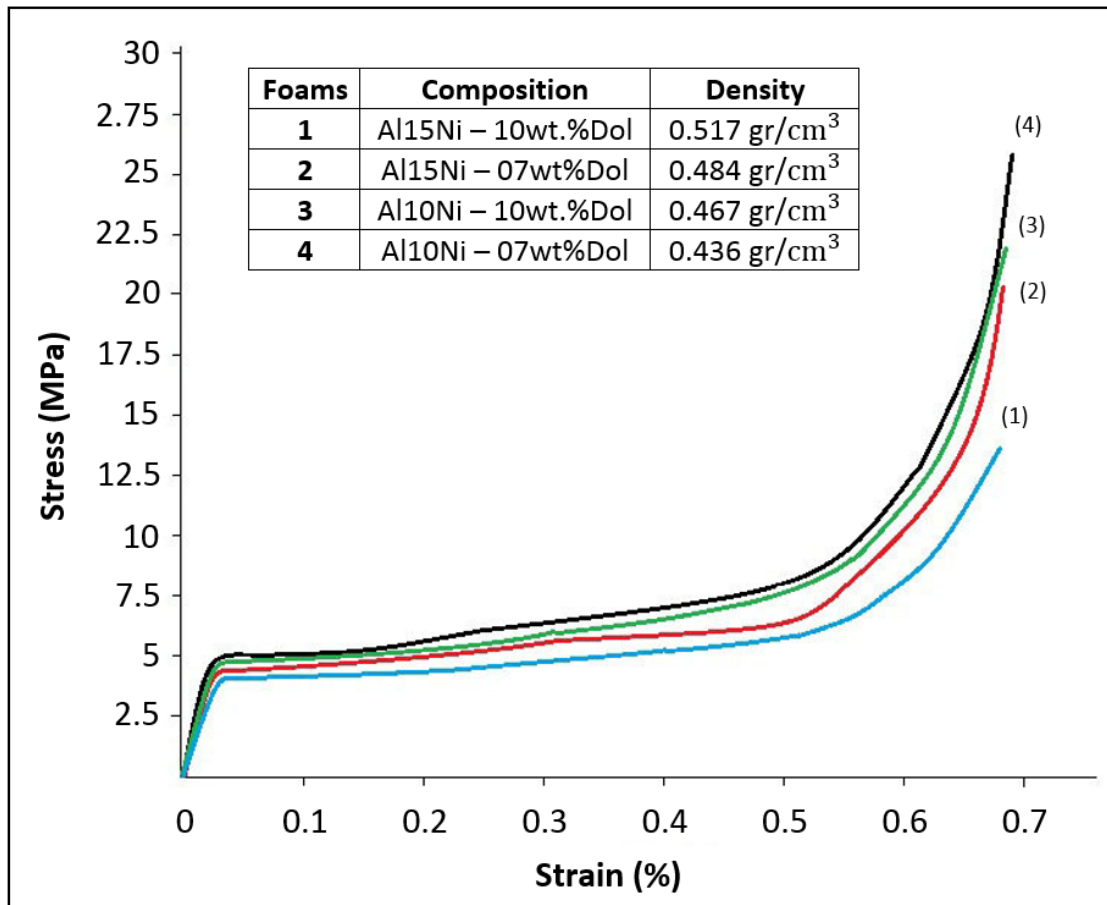


Fig. 6.2: Stress-Strain Curves of Al10Ni and Al15Ni with dolomite (7 and 10wt%)

The stress-strain curves (Fig. 6.2) present a typical behaviour exhibited by the metallic foams comprising of a maximum stress value, known as compressive strength (in this case ranging from 4.06 to 5.09 MPa – Table 6.1) beyond which the foams begin to collapse, followed by a stress “plateau” region in which successive internal cells slowly begin to deform and there after by a

steep increase in stress marked by an inflection in the stress-strain curve in which the cellular material begins to densify and cell rupture occurs. It is evident from Table 6.1 that the foams studied presented different densities attributable to variations in the samples selected in terms of composition and foams characteristics. However, the relative densities should represent only the physical characteristics of the obtained foams. It should be pointed out that density values are much lower than the ones found in the literature (~ 0.292) for studies carried out with the same foaming agent [32]. From Fig. 6.2 it can be seen that the foam with the largest density (Al-15Ni-10wt%Dol) was the first to experience the onset of densification and the foam with the smallest density (Al-10Ni-7wt%Dol) was the last. Even though the curves show only small dissimilarities, the compressive behavior of the foams are comparable. Using the peak method, the resultant plateau stress of 5.09 ± 0.08 MPa was obtained the start of densification strain of 0.61 ± 0.02 . Al-10Ni with 7wt% dolomite provided ideal results that were four times more effective compared with any other dolomite foams published in the literature [32,43].

Table 6.1: Density, relative density and compressive properties of the tested samples

Foam Matrix	Density (gr/cm³)	Relative Density	Plateau Stress (MPa)	Onset Densification Strain	Energy Absorption (MJ/m³)
Al15Ni + 10wt% Dol	0.51±0.06	0.18±0.02	3.76±0.13	0.50±0.08	0.47±0.31
Al15Ni + 07wt% Dol	0.48±0.02	0.15±0.01	4.69±0.11	0.56±0.07	0.75±0.18
Al10Ni + 10wt% Dol	0.46±0.01	0.13±0.01	4.79±0.06	0.59±0.03	0.83±1.85
Al10Ni + 07wt% Dol	0.43±0.03	0.11±0.01	5.09±0.08	0.61±0.02	0.94±1.82

This type of foams showed higher compression strength accompanied by smaller plateau regimes. The stress-strain behavior of foams from other studies experienced lower yield points and constant fluctuations in the energy absorption. These singularities were related to the local failure of cell walls [85]. Certainly, the use of dolomite to produce aluminum foams delivers a variety of cell shapes from ellipsoidal to spherical, but the Al-10Ni with 7wt% of dolomite, consistently exhibits uniformly spherical pores distributed throughout the foam. Multiple studies have shown that the mechanical behavior of foams is directly related to its equiaxed cell shape and thickness of its cell walls [86, 87, 88]. Nevertheless, in terms of cell size distribution, this has not been found to be such an influential factor being mostly dependant on cell morphology [87].

The energy absorption was calculated and is also summarize in Table 6.1. It is evident that the foam resulting from Al-10Ni-7wt%Dol absorbs higher energy than the other compositions. It is believed that this is related to the pore structure being uniformly distributed within the cellular material. Moreover, the energy absorption values obtained in this study are comparable or higher than values reported for most aluminum based foams elsewhere in the literature [32,43].

7. CONCLUSIONS

The central idea of this thesis has been to better understand and control the factors that influence dolomite ($\text{CaMg}(\text{CO}_3)_2$) as a foaming agent and to put forward a system that could improve foaming conditions for the production of aluminum foams. The use of a suitable metallic matrix for balancing temperatures and the modification of the conventional powder metallurgy route were the methods employed to obtain a highly porous structure.

- From this study, it was possible to conclude that, Al-Ni combinations deliver favorable semi-solid regions or formation of transient liquid phase which decreases the amount of gas loss during the foaming process. These alloys presented better viscosities than pure aluminum or other aluminum alloys for enclosing the carbon dioxide released from the decomposition of dolomite.
- It was shown that Al-10Ni and Al-15Ni are the most suitable alloys for the production of stable aluminum foams using a foaming agent with a high decomposition temperature such a dolomite. Al-10Ni provided the greatest results and is attributed to having enough viscosity in the melt for viable pore formation.

- An additional feature that Al-Ni alloys provide was an increase in the stability of the foam, attributed to the precipitation of the Al_3Ni intermetallic. The presence of a two phases (L+ Al_3Ni) while bubbles develop during foaming, reduces the surface tension providing greater stability and resistance to bubble collapse.
- From the experimental results it was found that by controlling the dolomite content the volume expansion can influence porosity levels and cell structure of the foam. A 7wt% concentration of dolomite exhibited the best results, releasing 0.02 moles of CO_2 during the foaming process.
- To produce aluminum foams using dolomite brings about a more gradual foaming process. The moderately slow decomposition kinetics of dolomite, compare to titanium hydride, develops stability and control over the level of porosity which can be achieved. Its low rate of thermal decomposition at high temperatures eliminates any prerequisite of processing or pretreating the foaming agent in order to postpone the beginning of thermal decomposition. For these reasons, dolomite is considered a cost-effective alternative as a foaming agent.
- Pore size analysis of the Al-10Ni with 7wt% of dolomite showed optimal results with high levels of porosity (~ 86%), elevated volume expansion (~ 244%) and semi-spherical pore morphology (~3 mm of diameter). They also exhibited high levels of pore nucleation and

low levels of pore coarsening and coalescence, all important factors for producing larger complex shapes.

- Integrating a partial-sintering step to the manufacturing process ensures minimum values of residual porosity in foamable precursors. This prior heat treatment allows rapid coalescence of metallic particles in the solid state. It causes an acceleration of particle bondings, an increase in the strength of the precursor, and promotes encapsulation of foaming gas.
- Subjecting a foamable precursor to partial-sintering not only allows pore growth according to the evolution of the two stages of dolomite decomposition but also to produce a level of expansion ten times higher than a precursor without heat treatment.
- In-situ observations of pre-heated precursors revealed that in order to obtain maximum values of theoretical density (99%) and to accelerate the sintering process, it only requires a holding time 15 minutes at 450°C. Although, holding times longer than 20 minutes increased the strength of the partially-sintered compact, they did not reach a greater volume of expansion or level of porosity.
- It was shown that Al-10Ni with 7wt% dolomite foams exhibited favorable characteristics for compressive strength and energy absorption. Values of the resultant plateau stress (5.09 ±0.08 MPa) and the amount of energy absorbed per volume (0.94±1.82 MJ/m³) were found

four times higher and effective compared with any other dolomite foams published in the literature

8. FUTURE WORK

To explore further the mechanical properties of the Al-Ni foams using dolomite as a foaming agent, especially acoustic properties, and energy absorption.

To discover and study different combination of metals as alloy matrices with even high melting temperatures, in order to develop other suitable systems for the production of foams with dolomite and minimize the gap of the decomposition temperature and the melting point of the metallic matrix. For example: Al-Mn, Al-Si.

The reproducibility of the foams should be further investigated in order to minimize defects of foaming and optimize foam uniformity to obtain comparable results in terms of compressive strengths.

The addition of lubricants to the original mixture with the objective of eliminating hot compaction to reduce cost reduction, in order to emphasize and further explore the partial-sintering step.

To investigate the viability of using the Al-Ni foam with dolomite as the foaming agent via PM for the fabrication of a heat exchanger and other applications.

9. REFERENCES

1. Banhart, J. *Manufacturing routes for metallic foams*. JOM, 2000, vol. 52, no 12, p. 22-27.
2. Kalpakjian, S.; Schmid, S. R. *Manufacturing Engineering and Technology*. Prentice Hall, 2014, p. 5-6.
3. Lefebvre, L.-P.; Banhart, J.; Dunand, D. *Porous metals and metallic foams: current status and recent developments*. Advanced Engineering Materials, 2008, vol. 10, no 9, p. 775-787.
4. Baumgärtner, F.; Duarte, I.I; Banhart, J. *Industrialization of powder compact foaming process*. Advanced Engineering Materials, 2000, vol. 2, no 4, p. 168-174.
5. Gergely, V.; Curran, D. C.; Clyne, T. W. *The FOAMCARP process: foaming of aluminium MMCs by the chalk-aluminium reaction in precursors*. Composites Science and Technology, 2003, vol. 63, no 16, p. 2301-2310.
6. Proa-Flores, P. *Aluminium foams fabricated by the PM route using nickel-coated titanium hydride powders of controlled particle size*. PhD Thesis, Department of Mining and Materials Engineering McGill University, Canada, 2010: p. 23-33.
7. Banhart, J. *Manufacture, characterisation and application of cellular metals and metal foams*. Progress in Materials Science, 2001, vol. 46, no 6, p. 559-632.
8. Andersen, O.; Waag, U.; Schneider, L.; Stephani, G.; & Kieback, B. *Novel metallic hollow sphere structures*. Advanced Engineering Materials, 2000, vol. 2, no 4, p. 192-195.

9. Volz, R. A. *Reticulated polyurethane foams and process for their production*. U.S. Patent Mar. 1995, no 3,171,820, 2.
10. Angel, S.; Bleck, W.; Harksen, S.; Scholz, P. F. *Functional and structural characteristics of metallic foams produced by the slip reaction foam sintering (srfs) - process*. Materials Science Forum. Trans Tech Publications, 2005, p. 39-46.
11. Tupil, S. P.; Büchner, K.; Lahmann, P.M. *Lamination of microcellular articles*. U.S. Patent Mayo 2001, no 6,235,380, 22.
12. Jin, I.; Kenny, Lorne D.; Sang, H. *Method of producing lightweight foamed metal*. U.S. Patent. Nov. 2000, no 4,973,358, 27.
13. Park, C.; Nutt, S. R. *PM synthesis and properties of steel foams*. Materials Science and Engineering: A, 2000, vol. 288, no 1, p. 111-118.
14. Liu, J.; Zou, S.; Li, S.; Liao, X.; Hong, Y.; Xiao, L.; Fan, J. *A general synthesis of mesoporous metal oxides with well-dispersed metal nanoparticles via a versatile sol-gel process*. Journal of Materials Chemistry A, 2013, vol. 1, no 12, p. 4038-4047.
15. Shapovalov, V.; Boyko, L. *Gasar—a new class of porous materials*. Advanced Engineering Materials, 2004, vol. 6, no 6, p. 407-410.
16. Hohlfeld, J.; Hannemann, C.; Vogel, R.; Hipke, T.; Neugebauer, R. *Alternative starting materials for the production of aluminum foam by the powder metallurgical process*. Production Engineering, 2011, vol. 5, no 1, p. 25-30.
17. Ashby, M. F.; Evans, A.; Fleck, N. A.; Gibson, L. J.; Hutchinson, J. W.; Wadley, H. N. *Metal foams: a design guide: Butterworth-Heinemann*, ISBN 0-7506-7219-6, Oxford, UK, 2000, Hardback, p. 251.

18. Degischer, H.; Kriszt, B. *Handbook of cellular metals*. Weinheim: Wiley-vch, 2002.
19. Kennedy, A. R. *Effect of compaction density on foamability of Al-TiH₂ powder compacts*. Powder Metallurgy, 2013, p. 451-452.
20. Asavavisithchai, S.; Kennedy, A. R. *The effect of compaction method on the expansion and stability of aluminium foams*. Advanced Engineering Materials, 2006, vol. 8, no 9, p. 810-815.
21. Matijasevic, B.; Banhart, J. *Improvement of aluminium foam technology by tailoring of blowing agent*. Scripta Materialia, 2016, vol. 54, no 4, p. 503-508.
22. Stanzick, H.; Wichmann, M.; Weise, J.; Helfen, L.; Baumbach, T.; Banhart, J. *Process control in aluminum foam production using real-time X-ray radioscopy*. Advanced Engineering Materials, 2012, vol. 4, no 10, p. 814-823.
23. Duarte, I.; Banhart, J. *A study of aluminium foam formation—kinetics and microstructure*. Acta Materialia, 2000, vol. 48, no 9, p. 2349-2362.
24. Banhart, J. *Metal foams: production and stability*. Advanced Engineering Materials, 2006, vol. 8, no 9, p. 781-794.
25. Clyne, T. W., et al. *Metal Matrix Composites and Metallic Foams: EUROMAT 99*. Vch Verlagsgesellschaft Mbh, 2000.
26. Alghamdi, A. *Collapsible impact energy absorbers: an overview*. Thin-walled structures, 2001, vol. 39, no 2, p. 189-213.
27. Srivastava, V. C.; Sahoo, K. L. *Processing, stabilization and applications of metallic foams*. Art of science. Materials Science, Poland, 2007, vol. 25, no 3, p. 733-753.

28. Rosen, M. J. *Micelle formation by surfactants*. Surfactants and Interfacial Phenomena, 2004, vol 4, p. 105-177.
29. Banhart, J. *Metal Foams: The mystery of stabilization*. MetFoam 2005. Kyoto, Japan.
30. Haesche, M.; Weise, J.; Garcia-Moreno, F.; & Banhart, J. *Influence of particle additions on the foaming behaviour of AlSi11/TiH₂ composites made by semi-solid processing*. Materials Science and Engineering: A, 2008, vol. 480, no 1, p. 283-288.
31. Babcsán, N.; Leitmeyer, D.; Banhart, J. *Metal foams—High temperature colloids: Part I. Ex situ analysis of metal foams*. Colloids and Surfaces A: Physicochemical and Engineering Aspects, 2005, vol. 261, no 1, p. 123-130.
32. Papadopoulos, D. P.; Omar, H., Stergioudi, F.; Tsipas, S. A.; Lefakis, H.; Michailidis, N. *A novel method for producing Al-foams and evaluation of their compression behavior*. Journal of Porous Materials. 2010, vol. 17, no: 6, p. 773-777.
33. Oak, S. M.; Kim, B. J.; Kim, W. T.; Chun, M. S.; Moon, Y. H. *Physical modeling of bubble generation in foamed-aluminum*. Journal of Materials Processing Technology, 2002, vol. 130, p. 304-309.
34. Vardumyan, L. E.; Khachatryan, H. L.; Harutyunyan, A. B.; Kharatyan, S. L. *Combustion synthesis of TiSi-based intermetallic foams using complex foaming agents*. Journal of Alloys and Compounds, 2008, vol. 454, no 1, p. 389-393.
35. Koizumi, T.; Kido, K.; Kita, K.; Mikado, K.; Gnyloskurenko, S.; Nakamura, T. *Effect of mass fraction of dolomite on the foaming behavior of AlSiCu alloy foam by powder metallurgy route*. Metallurgical and Materials Transactions A, 2012, vol. 43, no 11, p. 4377-4382.

36. Putz H.; Brandenburg K. Pearson's Crystal Data, Crystal structure database for inorganic compounds, CD-ROM software version 1.3.
37. Kennedy, A. R.; Lopez, V. H. *The decomposition behavior of as-received and oxidized TiH₂ foaming-agent powder*. Materials Science and Engineering: A, 2003, vol. 357, no 1, p. 258-263.
38. Paulin, I. *Synthesis and characterization of Al foams produced by powder metallurgy route using dolomite and titanium hydride as a foaming agents*. Materials and Technology, 2014, vol. 48, no 6, p. 943-947.
39. Gnyloskurenko, S. V.; Koizumi, T.; Kita, K.; Nakamura, T. *Aluminum metallic foams made by carbonate foaming agents*. Environmental Resources Engineering. 2013, vol. 60, no 1, p. 5-12.
40. Nakamura, T.; Gnyloskurenko, S. V.; Sakamoto, K.; Byakova, A. V.; Ishikawa, R. *Development of new foaming agent for metal foam*. Materials Transactions, 2002, vol. 43, no 5, p. 1191-1196.
41. Haesche, M.; Lehmhus, D.; Weise, J.; Wichmann, M.; Mocellin, I. C. M. *Carbonates as foaming agent in chip-based aluminium foam precursor*. Journal of Materials Science and Technology, 2010, vol. 26, no 9, p. 845-850.
42. Dobrzański, L. A.; Labisz, K.; Olsen, A. *Microstructure and mechanical properties of the Al-Ti alloy with cerium addition*. Journal of Achievements in Materials and Manufacturing Engineering, 2009, vol. 37, no 2, p. 622-629.
43. Papadopoulos, D. P.; Omar, H.; Stergioudi, F.; Tsipas, S. A.; Michailidis, N. *The use of dolomite as foaming agent and its effect on the microstructure of aluminium metal foams—*

- Comparison to titanium hydride*. Colloids and Surfaces A: Physicochemical and Engineering Aspects, 2011, vol. 382, no 1, p. 118-123.
44. Koizumi, T.; Kido, K.; Kita, K.; Mikado, K.; Gnyloskurenko, S.; Nakamura, T. *Method of preventing shrinkage of aluminum foam using carbonates*. Metals, 2011, vol. 2, no 1, p. 1-9.
 45. Varuzan K.; Sreco D. S.; Irena P.; Uros K.; Monika J. *Effect of a foaming agent and its morphology on the foaming behaviour, cell-size distribution and microstructural uniformity of closed-cell aluminium foams*. Materials and Technology, 2012, vol 46, no 3, p.233–238.
 46. EG, Materials and aerospace corporation, *Duocel Aluminum Foam*. California, 2015, p.2
 47. Varuzan K.; Sreco D. S.; Irena P.; Uros K.; Monika J. *Synthesis and characterisation of closed cells aluminium foams containing dolomite powder as foaming agent*. Materials and Technology 2010, vol. 44, no 6, p. 363-371.
 48. Szajnar, J.; Wróbel, T. *Inoculation of primary structure of pure aluminium*. Journal of Achievements in Materials and Manufacturing Engineering, 2007. Vol 20, p. 283-286.
 49. Bishop, D. P.; Cahoon, J. R.; Chaturvedi, M. C.; Kipouros, G. J.; Caley, W. F. *Diffusion-based micro-alloying of aluminium alloys by powder metallurgy and reaction sintering*. Journal of Materials Science, 1998, vol. 33, no 15, p. 3927-3934.
 50. Alizadeh, M.; Mohammadi, G.; Fakhrabadi, G. H. A.; Aliabadi, M. M. *Investigation of chromium effect on synthesis behavior of nickel aluminide during mechanical alloying process*. Journal of Alloys and Compounds, 2010, vol. 505, no 1, p. 64-69.

51. Enayati, M. H.; Sadeghian, Z.; Salehi, M. A. H. D. I.; Saidi, A. *The effect of milling parameters on the synthesis of Ni₃Al intermetallic compound by mechanical alloying*. Materials Science and Engineering: A, 2004, vol. 375, p. 809-811.
52. Yoon, E. H.; Hong, J. K.; Hwang, S. K. *Mechanical alloying of dispersion-hardened Ni₃Al-B from elemental powder mixtures*. Journal of Materials Engineering and Performance, 1997, vol. 6, no 1, p. 106-112.
53. Shi, D.; Wen, B., Melnik, R.; Yao, S.; Li, T. *First-principles studies of Al-Ni intermetallic compounds*. Journal of Solid State Chemistry, 2009, vol. 182, no 10, p. 2664-2669.
54. Nash P.; Singleton M.F.; Murray J.L. Al-Ni (*Aluminum-Nickel*), *Phase Diagrams of Binary Nickel Alloys*, P. Nash, ed., ASM International, Materials Park, OH, 1991, pp. 3-11
55. Brunelli, K.; Peruzzo, L.; Dabala, M. *The effect of prolonged heat treatments on the microstructural evolution of Al/Ni intermetallic compounds in multi layered composites*. Materials Chemistry and Physics, 2015, vol. 149, p. 350-358.
56. Baumeister, J.; Banhart, J.; Weber, M. *Aluminium foams for transport industry*. Materials and Design, 1997, vol. 18, no 4, p. 217-220.
57. Banhart, J.; Seeliger, H.-W. *Aluminium foam sandwich panels: Manufacture, metallurgy and applications*. Advanced Engineering Materials, 2008, vol. 10, no 9, p. 793-802.
58. Gibson, L. J. *Mechanical behavior of metallic foams*. Annual review of Materials Science, 2000, vol. 30, no 1, p. 191-227.

59. Benouali, A. H.; Froyen, L.; Delerue, J. F.; Wevers, M. *Mechanical analysis and microstructural characterisation of metal foams*. Materials Science and Technology, 2002, vol. 18, no 5, p. 489-494.
60. Banhart, J.; Baumeister, J.; Weber, M. *Metal foams near commercialization*. Metal Powder report, 1997, vol. 53, p. 38.
61. Arun Negi, V.S.R.; Dashrath S.; Himanshu P. *Compressive behaviour of aluminium foam prepared by melts route method by different addition of nickel particles*. International Journal of Mathematics and Physical Sciences Research, 2015. 3(1): p. 1-8.
62. Calliste R.; William D.; Rethwisch, D. G. *Fundamentals of materials science and engineering: an integrated approach*. John Wiley & Sons, 2012.
63. Ogorkiewicz, R. M.; Mucci, P. E. R. *Testing of fibre-plastics composites in three-point bending*. Composites, 1971, vol. 2, no 3, p. 139-145.
64. Fuganti, A.; Lorenzi, L.; Gronsund, A.; Langseth, M. *Aluminum foam for automotive applications*. Advanced Engineering Materials, 2011, vol. 2, no 4, p. 200-204.
65. Lafrance, M. *The reactive stabilisation of Al-Zn-X foams via the formation of a transient liquid phase using the powder metallurgy approach*. Department of mining and materials engineering McGill University, Canada, 2012, p. 60-61.
66. Šalák, A.; Vasilko, K.; Selecká, M.; Danninger, H. Production of sintering components. Journal of Materials Processing Technology, 2006, vol. 176, no 1, p. 62-69.

67. Esmaeelzadeh S.; Simchi A.; Lehemus D. *Effects of ceramic particle addition on the foaming behaviour, cell structure and mechanical properties of P/M AlSi7 foam*. Materials Science and Engineering A, 2006, vol. 424, p. 290-299.
68. Wubben T.; Stanzick H.; Banhart J.; Odenbach S. *Stability of metallic foams studied under microgravity*. Journal of Physics: Condensed Matter. 2009, vol. 14, p. S-427-S433.
69. Dudka A.; Garcia-Moreno F.; Wanderka N.; Banhart J. *Structure and distribution of oxides in aluminum foam*. Acta Materialia. 2008, vol. 56, p. 3990-4001.
70. Korner C. *Foam formation mechanisms in particle suspensions applied to metal foams*. Materials Science and Engineering A. 2008, vol. 495, p. 227-235.
71. Saadatfar M.; Garcia-Moreno, F.; Hutzler S.; Sheppard A. P.; Knackstedt M. A. *Imaging of metallic foams using X-ray micro-CT*. Colloids and Surfaces A: Physicochemical and Engineering Aspects. 2009, vol. 344, p. 107-112.
72. Karsu N. D.; Yuksel S.; Guden M. *Foaming behaviour of Ti6Al4V particle-added aluminum powder compacts*. Journal of Materials Science. 2009, vol. 44, p. 1494-1505.
73. Montanini R. *Measurement of strain rate sensitivity of aluminum foams for energy dissipation*. International Journal of Mechanical Sciences. 2005, vol. 47, p. 26-42.
74. Helwig, H. M.; Garcia-Moreno J.; Banhart J. *A study of Mg and Cu additions on the foaming behaviour of Al-Si alloys*. Journal of Materials Science. 2011, vol. 46, p. 5227-5236.

75. Adachi H.; Itaka W.; Aida, T.; Osamura K.; Imaoka M.; & Kusui, J. *Microstructure and mechanical properties of ternary intermetallic compound dispersed P/M Al-Mn-X-Zr (x=Cu,Ni) alloys*. Transactions of the Indian Institute of Metals, 2009, vol 62, no 2, p. 163-167.
76. Clyne, T.W.; Frantisek S. *Metal matrix composites and metallic foams: EUROMAT 99*. 2000, vol 5, p. 3-13.
77. Banhart, J. *Light-Metal Foams—History of Innovation and Technological Challenges*. Advanced Engineering Materials. 2013, vol 15, no 3, p. 82-111.
78. Lázaro J.; Solórzano E.; Rodríguez-Pérez M.A.; Rämér O.; García-Moreno F.; Banhart J. *Heat treatment of aluminium foam precursors: effects on foam expansion and final Cellular structure*. Procedia Materials Science, 2014, vol. 4, p. 287-292.
79. Baumeister J.; Schrader H.; *Verfahren zur Herstellung aufschäumbarer Metallkörper und Verwendung derselben*. German Patent, 1992, vol. 41, no 01, p. 630.
80. Haul R.; Heystek H. *Differential thermal analysis of the dolomite decomposition*. Am Mineral. 1995, p.166-179.
81. Blackford J.R. *Sintering and microstructure of ice: a review*. Journal of Physics D: Applied Physics. 2007, Vol 40, no: 21, p. R355.
82. Blazy J. S.; Marie-Louise A.; Forest S.; Chastel Y.; Pineau A.; Awade A.; Grolleron, C.; Moussy, F. *Deformation and fracture of aluminium foams under proportional and non proportional multi-axial loading: statistical analysis and size effect*. International Journal of Mechanical Sciences. 2004, vol 46, no 2, p. 217-244.

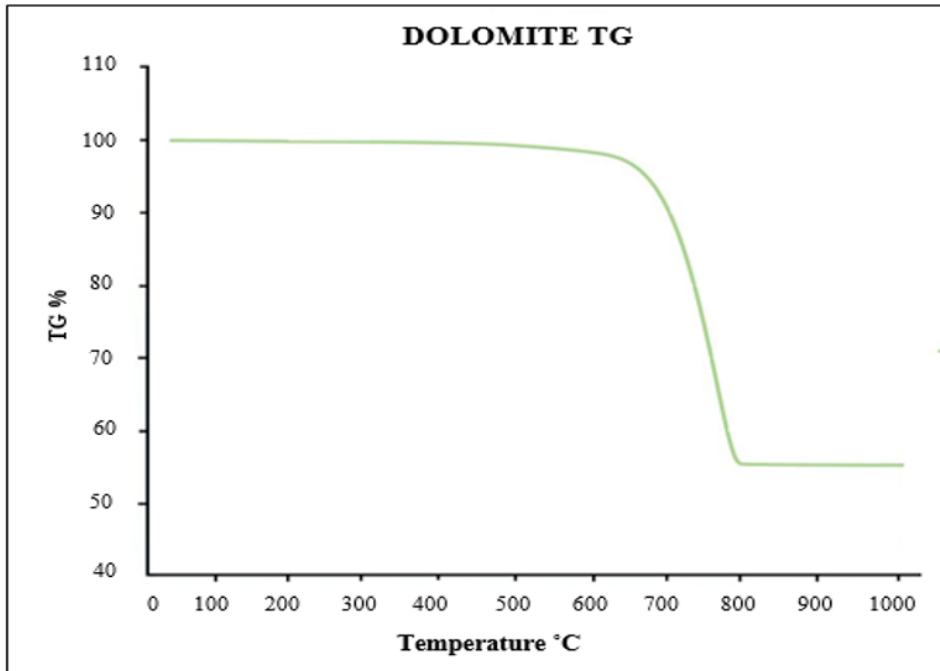
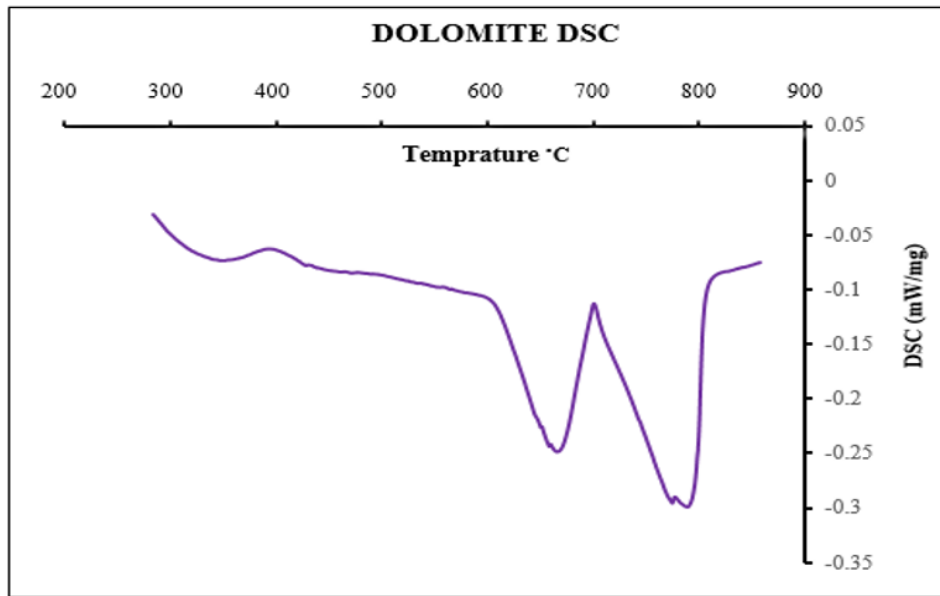
83. Banhart J.; Baumeister J.; Weber M. *Powder metallurgical technology for the production of metallic foams*. Proceedings of the European Conference on Advanced PM Materials, Birmingham. 1995.
84. Bouche K.; Barbier F.; Coulet A. *Phase formation during dissolution of nickel in liquid aluminium*. Zeitschrift für Metallkunde. 1997, vol 88.6, p.446-451.
85. Bart-Smith H.; Bastawros A. F.; Mumm D. R.; Evans A. G.; Sypeck D. J.; Wadley H. N. G. *Compressive deformation and yielding mechanisms in cellular Al alloys determined using X-Ray tomography and surface strain mapping*. Acta Materialia, 1998, vol 46, no 10, p. 3583-3592.
86. Evans A. G.; Hutchinson J. W.; Ashby M. F. *Multifunctionality of cellular metal systems*. Progress in Materials Science. 2009, vol 43, no 3, p. 171-221.
87. Sugimura Y.; Meyer J.; He M. Y.; Bart-Smith H. *On the mechanical performance of closed cell Al alloy foams*. Acta Materialia, 2012, vol 45, no 12, p. 5245-5259.
88. Markaki A.E.; Clyne T.W. *The effect of cell wall microstructure on the deformation and fracture of aluminium-based foams*. Acta Materialia. 2001, Vol 49, Issue 9, p.1677–1686
90. Angelo P.C.; Ramayyar S. *Powder metallurgy: science, technology and applications*. 2PHI learning Pvt. Ltd. 2008, p. 21-23.
91. Gunasekaran S.; Anbalagan G. *Thermal decomposition of natural dolomite*. Bulletin of Materials Science. 2007, vol 30, no 4, p. 339-344.

This page is intentionally left blank

APPENDIX A

DOLOMITE

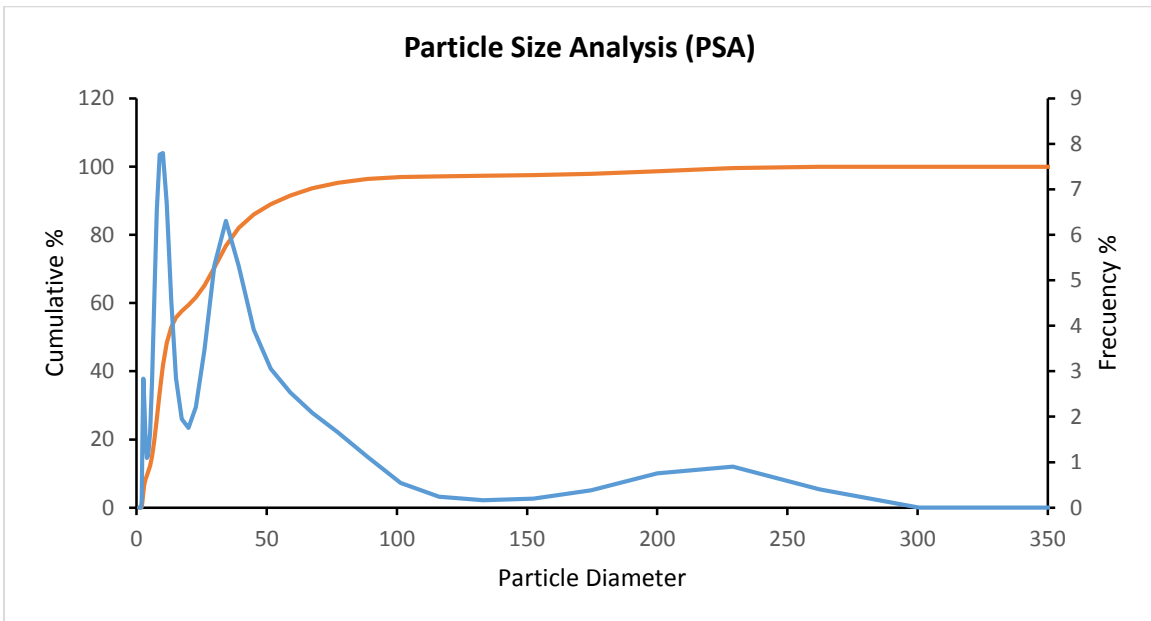
WEIGHT LOSS AND DECOMPOSITION ANALYSIS



APPENDIX B

PARTICLE SIZE ANALYSIS (PSA) OF DOLOMITE

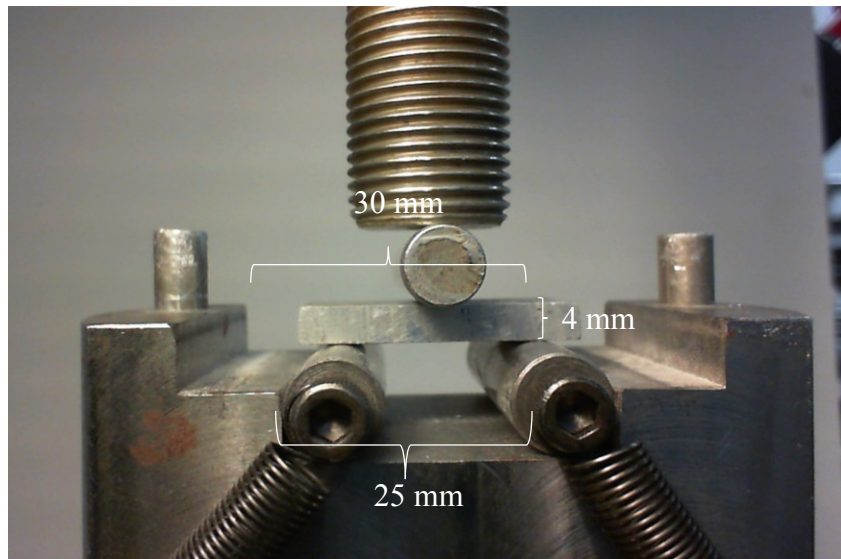
Median Size	12.16308(μm)
Mean Size	25.91740(μm)
Variance	1211.7(μm^2)
Std.Dev.	34.8092(μm)
Mode Size	9.3480(μm)
Geo.Mean Size	15.0293(μm)
Geo.Variance	1.5692(μm^2)
Skewness	3.6488
Kurtosis	19.1453
Diameter on Cumulative %	(2)10.00 (%) - 4.1869(μm) (4)30.00 (%) - 8.2505(μm) (6)60.00 (%) - 20.6029(μm) (9)90.00 (%) - 54.1992(μm)



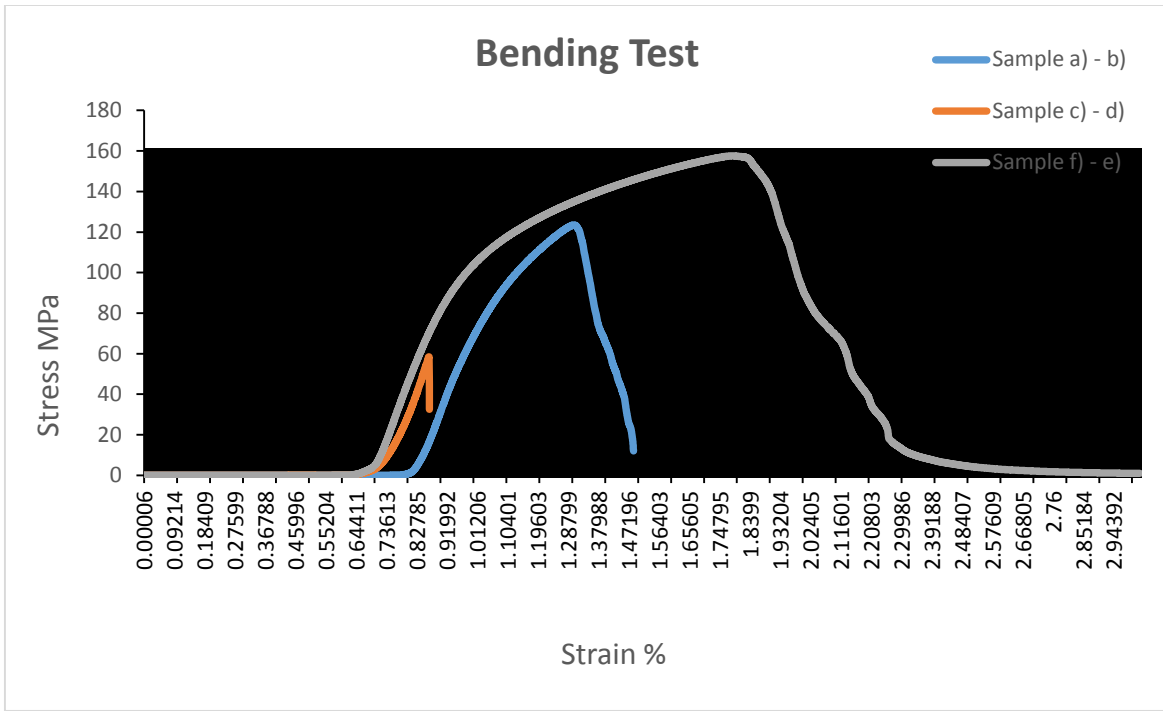
COMPACTS-FRACTURE SURFACE

BENDING TEST

Set up of the three-point bending test and the dimensions of the all the samples (30x4x15). After completing the test it was analyzed and evaluated the data which are summarized in the following table.

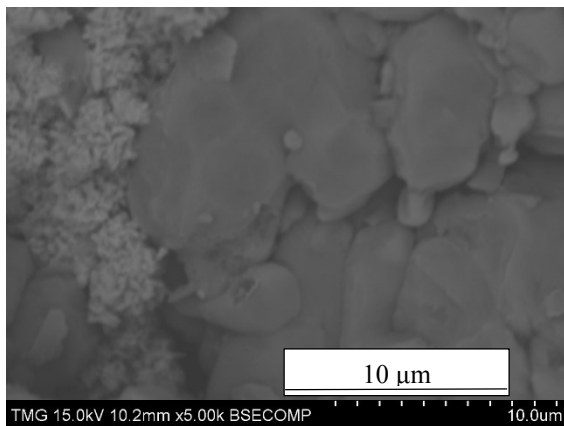
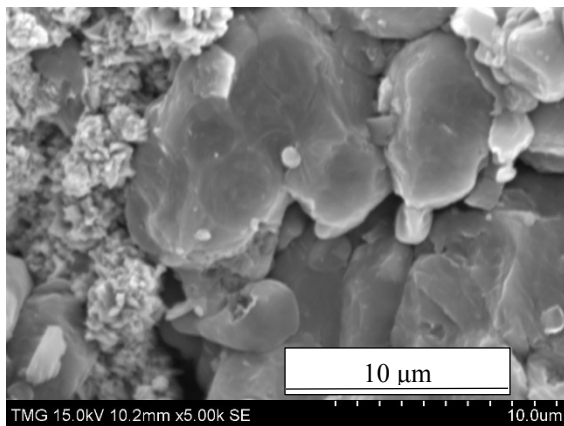
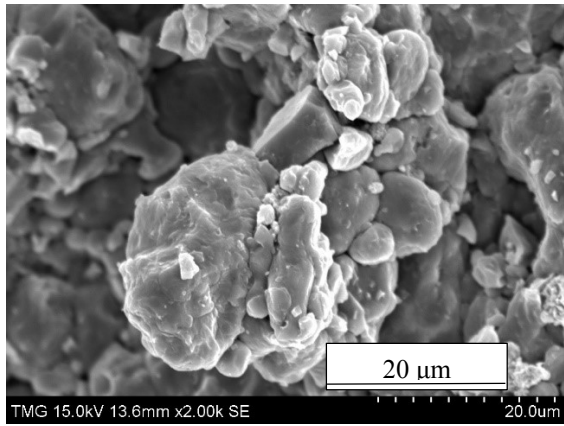
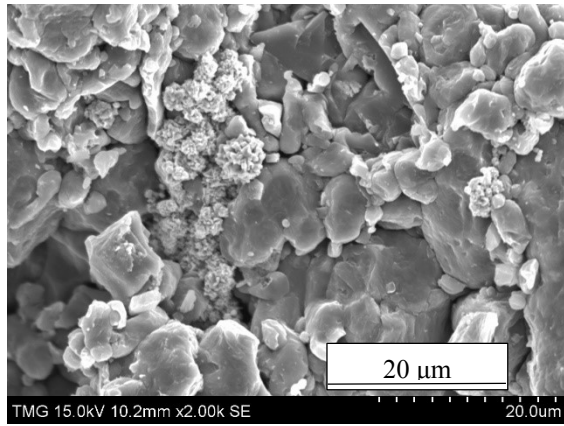
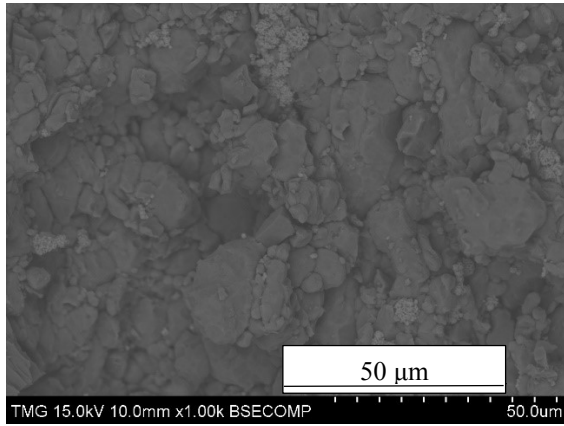
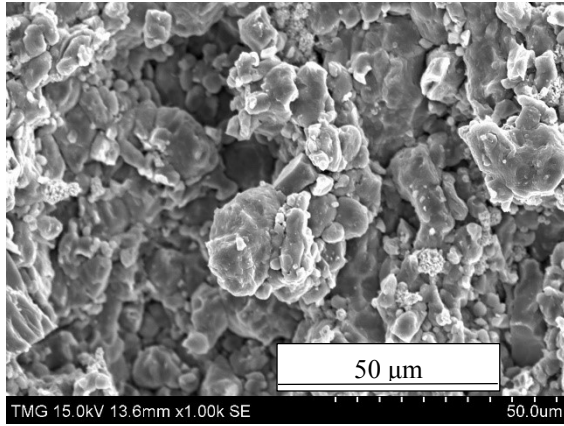


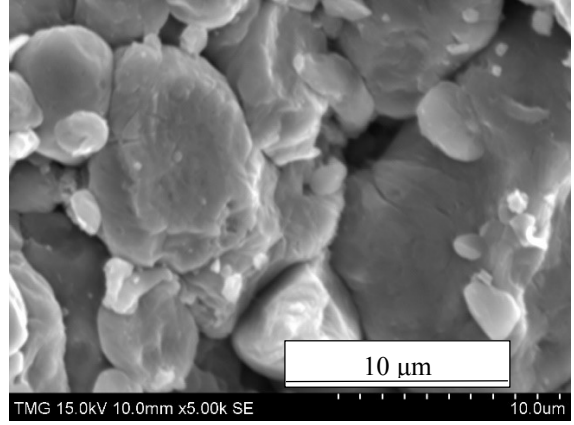
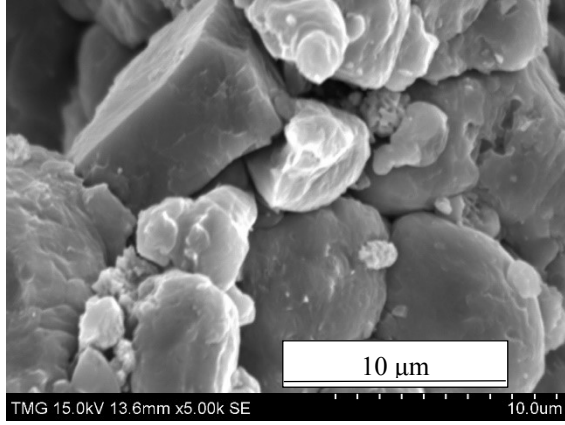
Three Point Bending Results				
Number	Density	Treatment	Minimum Load Average	Stress
			(N)	(MPa)
Sample a) - b)	98%	No	749	58.47
Sample c) - d)	98%	Yes (15min-400C)	1580	123.47
Sample e) - f)	98%	Yes (20min-400C)	2018	157.63



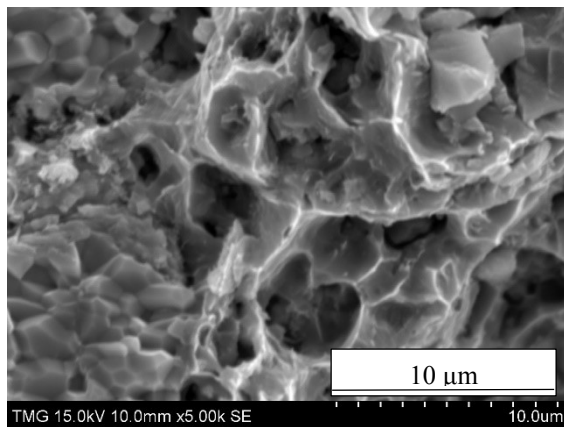
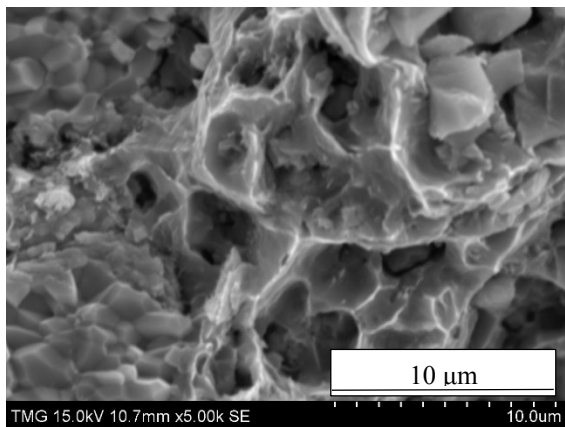
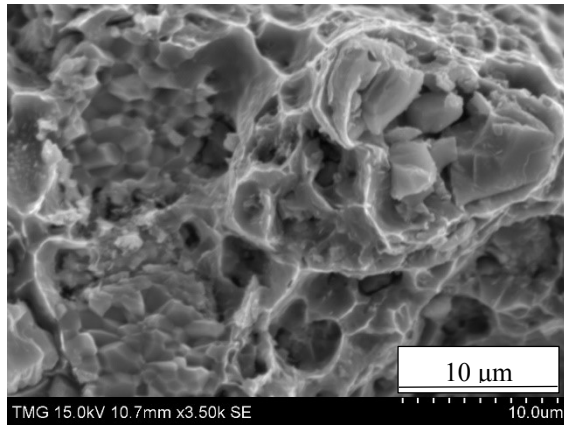
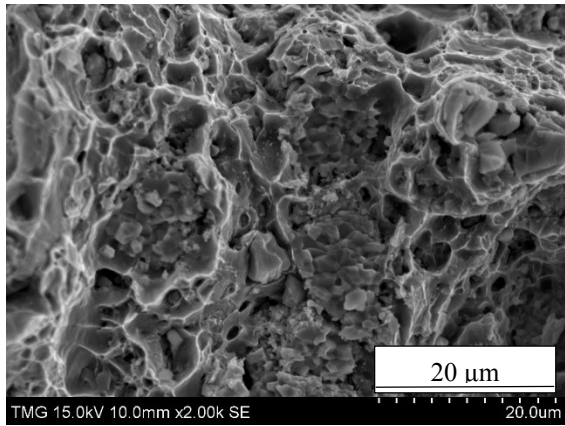
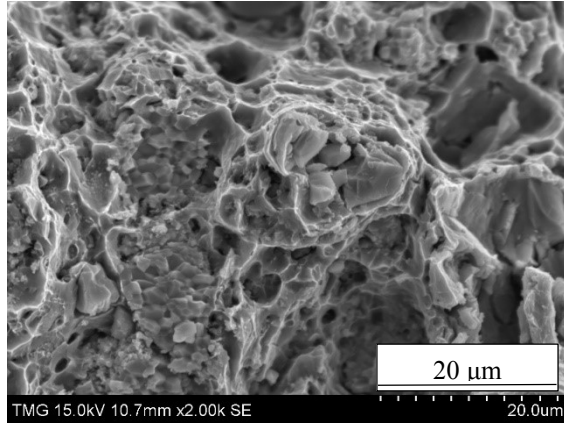
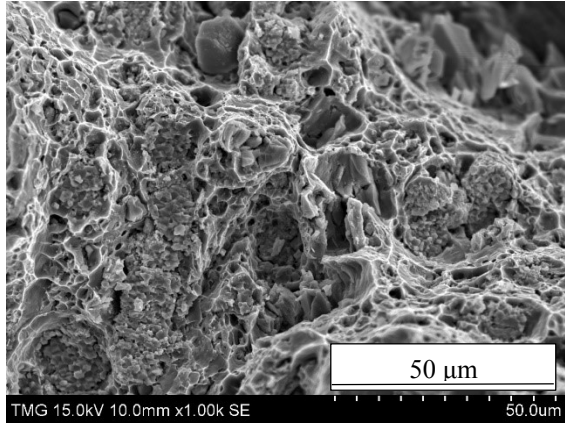
SURFACE FRACTURE ANALYSIS

Sample a) - b)

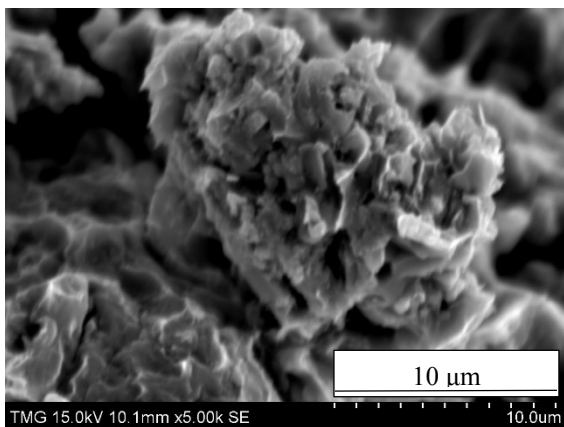
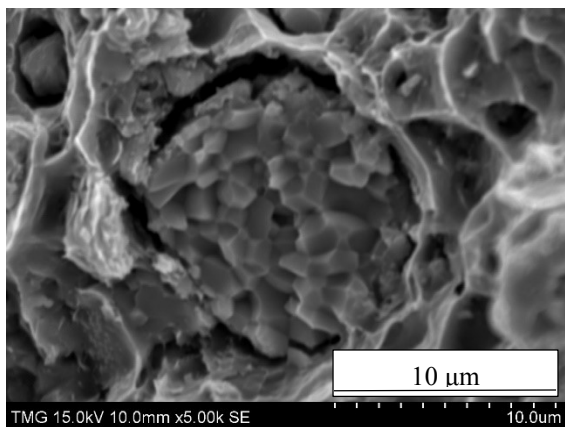
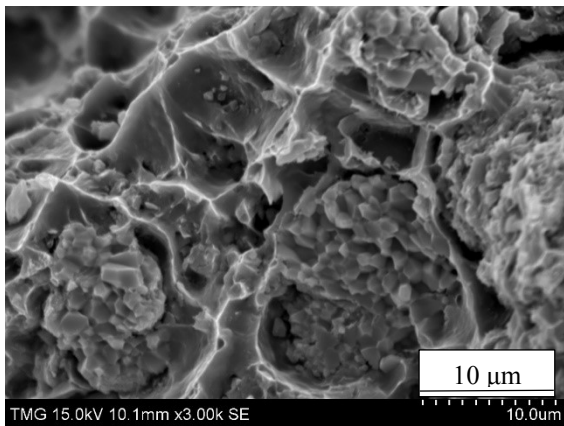
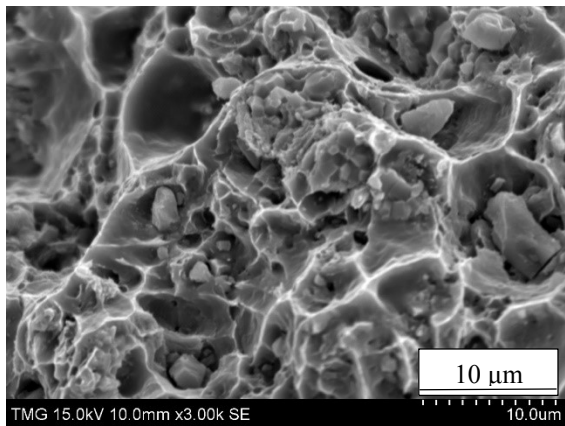
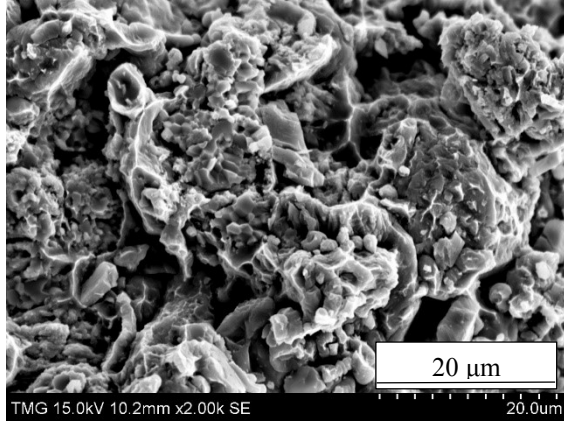
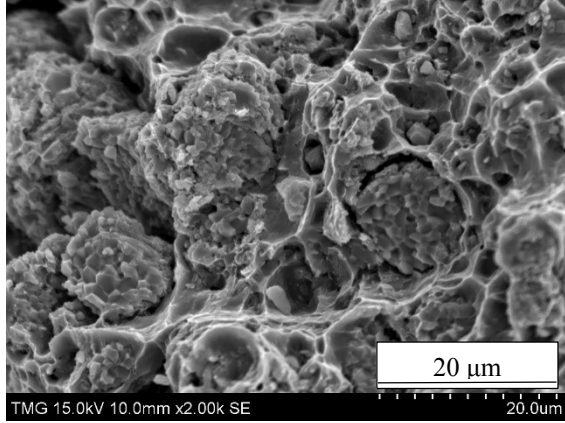




Sample c) - d)



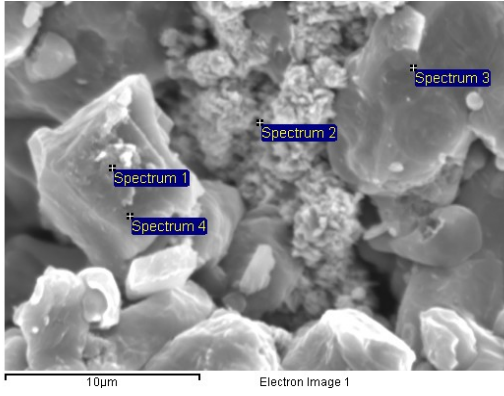
Sample e) - f)



POINT AND LINE SCAN OF THE SURFACE FRACTURES

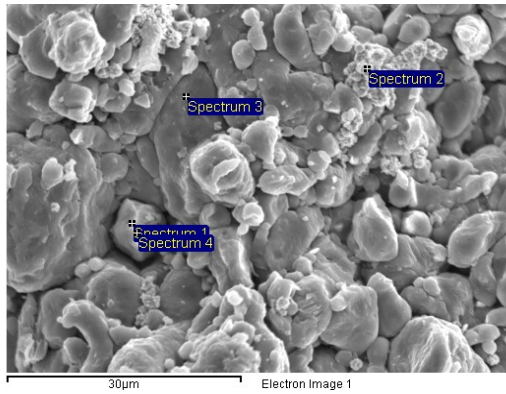
Identification of materials- chemical composition

Sample a) - b)



Spectrum	C	O	Mg	Al	Ca	Ni
Spectrum 1	18.6	58.1	10.4	2.36	10.1	0.31
Spectrum 2		5.7	1.25	21.8	0.58	70.5
Spectrum 3		3.2		95.4		1.29
Spectrum 4	18.7	55.9	11.5	1.48	12.6	0.38
Max.	18.7	58.1	11.5	95.4	12.6	70.5
Min.	18.6	3.29	1.25	1.48	0.58	0.31

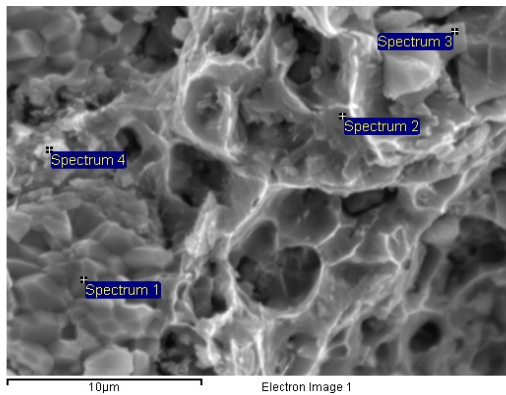
All results in atomic%



Spectrum	C	O	Al	Ni
Spectrum 1			10.51	87.45
Spectrum 2	33.84	2.96	9.58	53.61
Spectrum 3	20.93	2.01	76.51	0.54
Spectrum 4	20.93	2.01	76.51	0.54
Max.	33.84	10.51	87.45	53.61
Min.	20.93	2.01	9.58	0.54

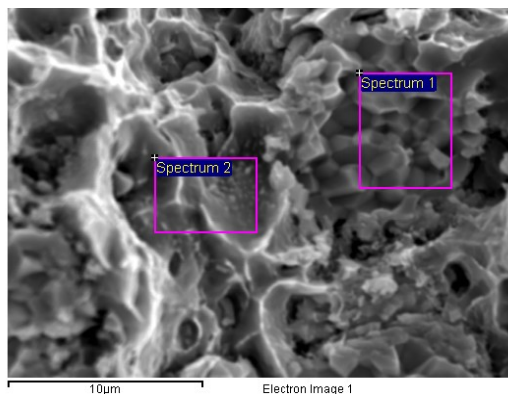
All results in atomic%

Sample c) - d)



Spectrum	C	O	Mg	Al	Ca	Ni
Spectrum 1	25.2	1.23		56.0		17.5
Spectrum 2	11.2	2.11		85.5		1.11
Spectrum 3	25.7	46.6	6.68	14.2	6.46	0.24
Spectrum 4	21.8	4.90		56.6	0.13	16.5
Max.	25.7	46.6	6.68	85.5	6.46	17.5
Min.	11.2	1.23	6.68	14.2	0.13	0.24

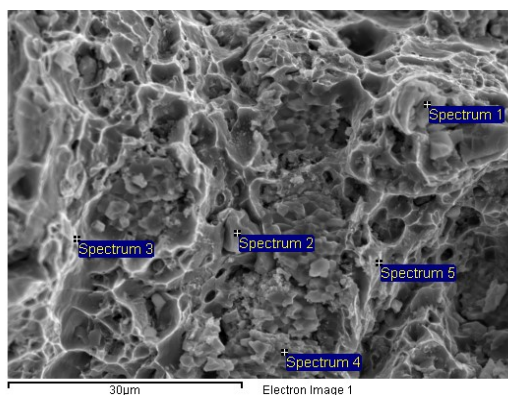
All results in atomic%



Spectrum	C	O	Al	Ni
Spectrum 1	21.31	1.62	55.84	21.23
Spectrum 2		4.33	94.46	1.21
Max.	21.31	4.33	94.46	21.23
Min.	21.31	1.62	55.84	1.21

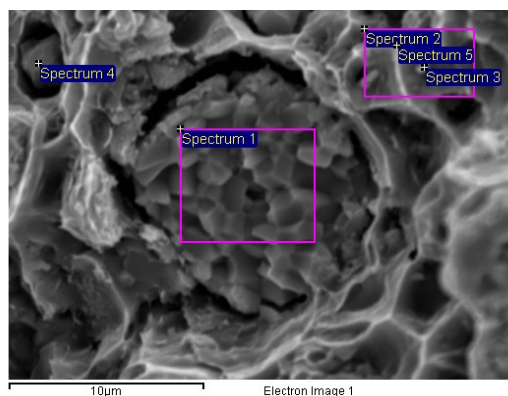
All results in atomic%

Sample e) - f)



Spectrum	C	O	Mg	Al	Ca	Ni
Spectrum 1	15.5	33.9	11.5	18.2	19.9	0.77
Spectrum 2		66.3	11.8	10.5	10.7	0.62
Spectrum 3		5.39		91.5		3.09
Spectrum 4	20.4	1.66		58.5		19.3
Spectrum 5	20.2	4.88	0.26	73.7	0.26	0.66
Max.	20.4	66.3	11.8	91.5	19.9	19.3
Min.	15.5	1.66	0	10.5	0.26	0.62

All results in atomic%



Spectrum	C	O	Mg	Al	Ca	Ni
Spectrum 1	17.9	1.64		58.6		21.7
Spectrum 2	18.7	4.66		75.3	0.22	1.07
Spectrum 3	16.5	4.50		78.3		0.61
Spectrum 4	22.8	24.6	6.52	33.6	10.2	2.15
Spectrum 5	29.3	6.25		63.3	0.21	0.79
Max.	29.3	24.6	6.52	78.3	10.2	21.7
Min.	16.5	1.64	6.52	33.6	0.21	0.61

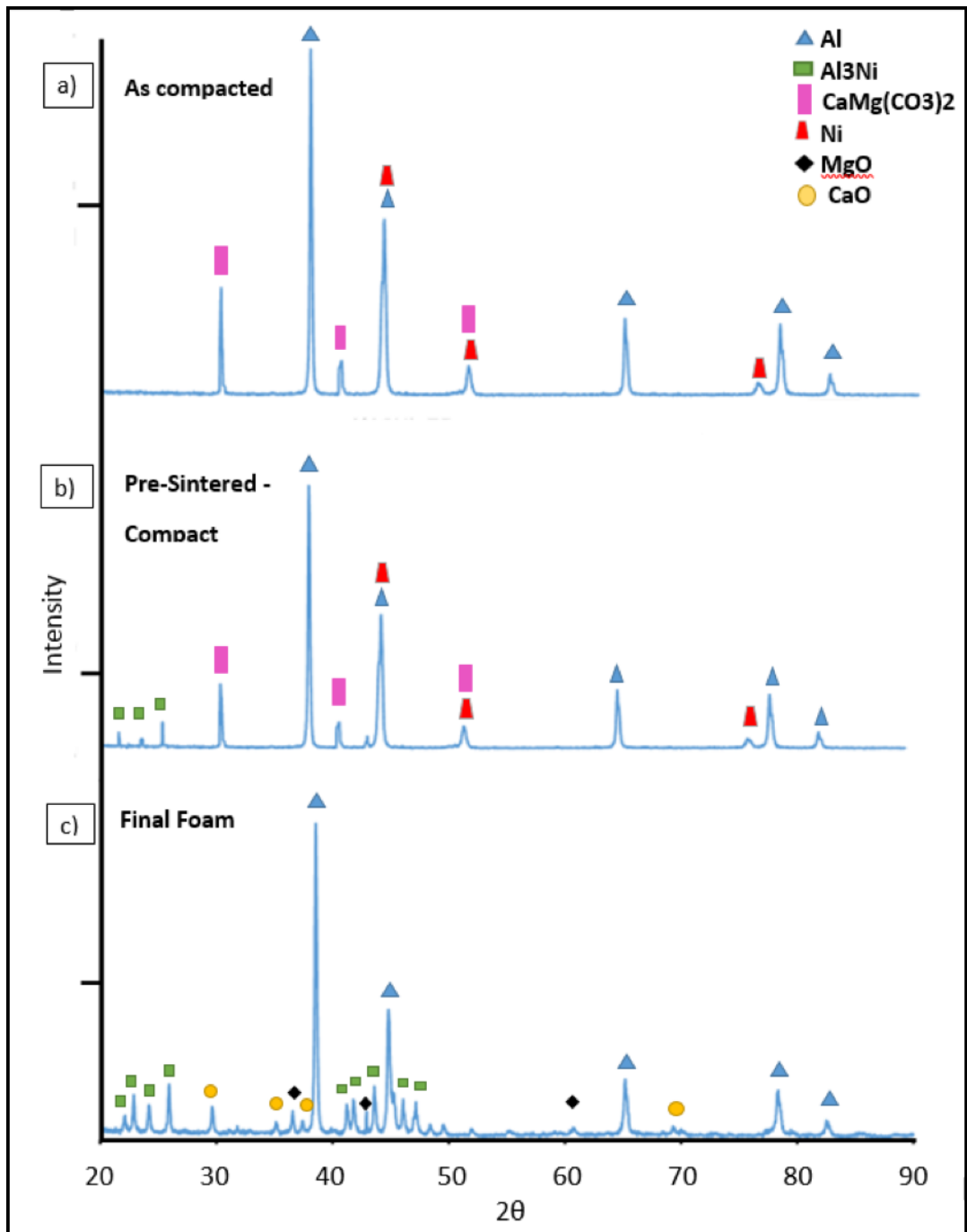
All results in atomic%

APPENDIX D

MORPHOLOGY-FOAMS

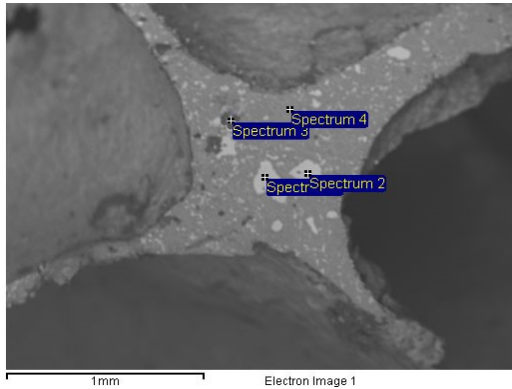
Additional XRD and EDS analyses shown above provide additional information regarding different phases obtained in the Al-10Ni composition from the “as-compacted” (a) specimen to the “partially-sintered” (b) and finally to the cellular material obtained (c).

As it can be observed the “as-compacted” sample showed only a combination of the metals in the elemental state and dolomite whereas upon partial-sintering the appearance of the intermetallic phase Al_3Ni is to be noted. Finally, in the obtained foam the intermetallic phase is further confirmed as it appears at the expense of Ni, in addition to MgO and CaO both resulted from dolomite decomposition.



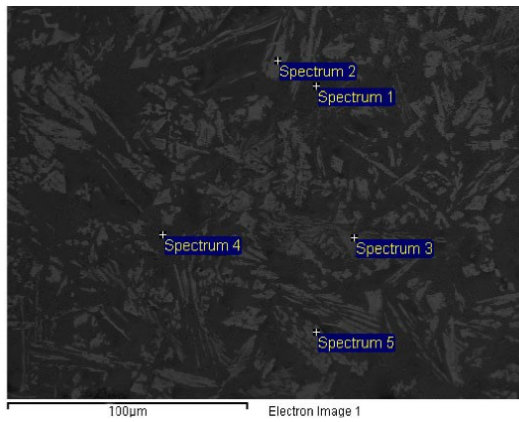
Phase identification of the “as-compacted” (a) partially-sintered (b) and the cellular material (c) of Al-10Ni with 7wt% dolomite

EDS analysis



Spectrum	Mg	C	O	Ca	Al	Ni
Spectrum 1					74.11	25.89
Spectrum 2		1.00			74.25	24.75
Spectrum 3	7.31	9.55	36.12	15.36	27.53	4.13
Spectrum 4		4.21	8.35	25.55	64.18	1.92

All results in atomic%

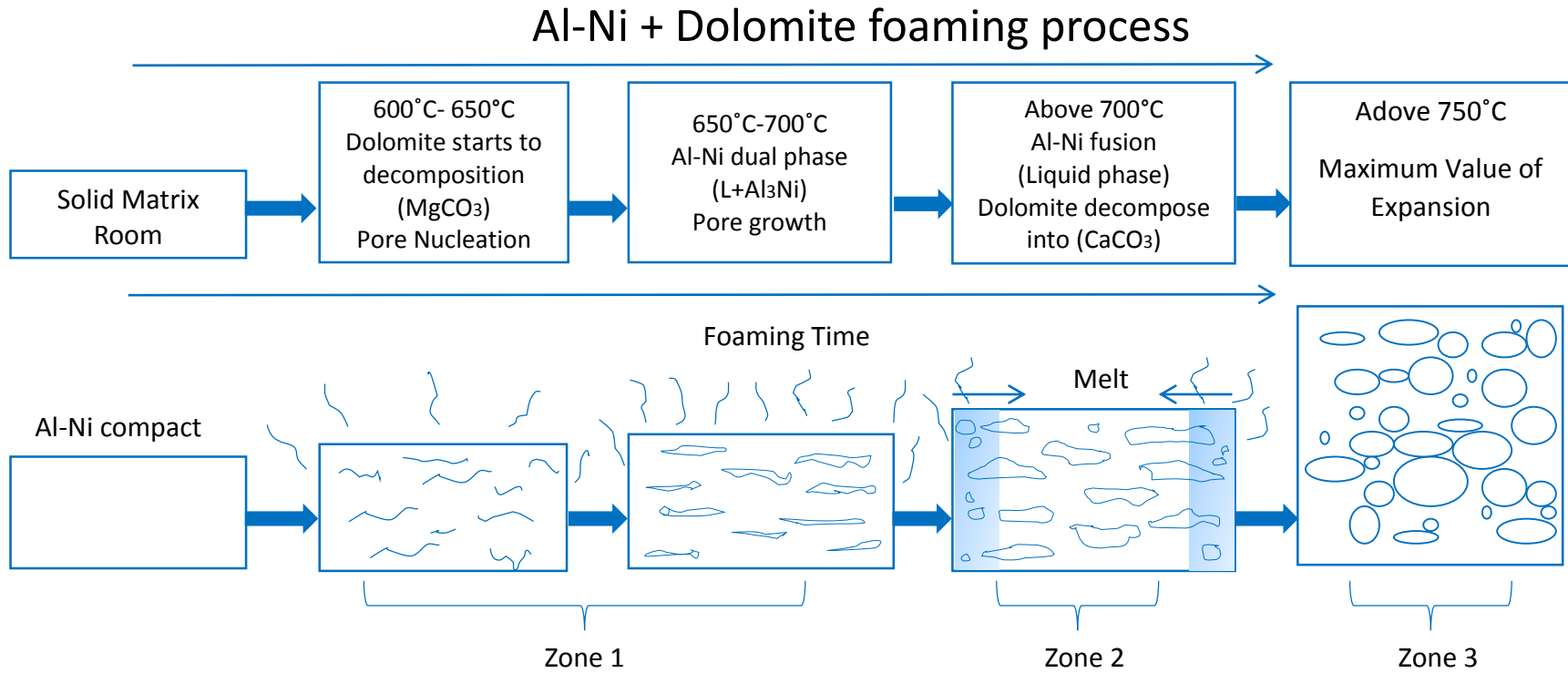


Spectrum	Ca	O	C	Al	Ni
Spectrum 1	32.16	34.01		31.14	2.69
Spectrum 2			4.6	71.55	23.85
Spectrum 3	1.08	0.86		73.54	24.51
Spectrum 4	1.16	4.61	0.35	92.3	1.58
Spectrum 5	32.99	32.07		31.37	3.58

All results in atomic%

APPENDIX E

Foaming Process of Al-Ni matrix vs pure Al matrix



Pure Al + Dolomite foaming Process

